Active Galactic Nuclei (AGN)

Itziar Aretxaga (itziar@inaoep.mx)
38th ISYA, Tehran, August 2016

Lecture 1: taxonomy

- Classification of AGN
- Multifrequency detection of nuclear activity
- Energetics
- Unification

Lecture 2: the role of BHs in AGN, and of AGN in galaxy formation and evolution

- Basic concepts of the standard model of AGN
- Evidence for BHs in AGN
- Methods to weight a BH in an AGN
- Demographics of QSOs and BHs
- QSOs in the context of galaxy formation and evolution

The standard model of AGN

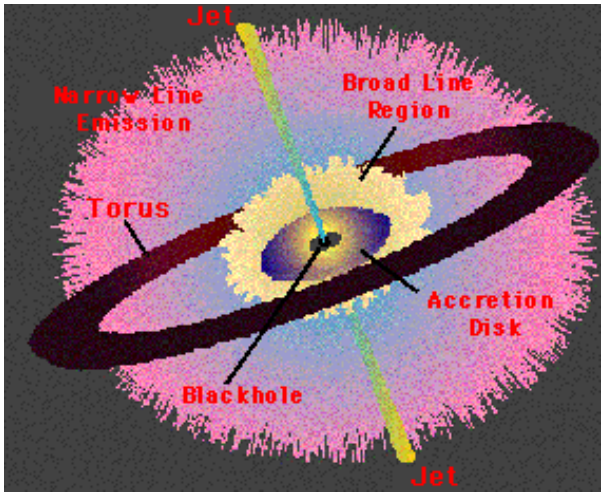

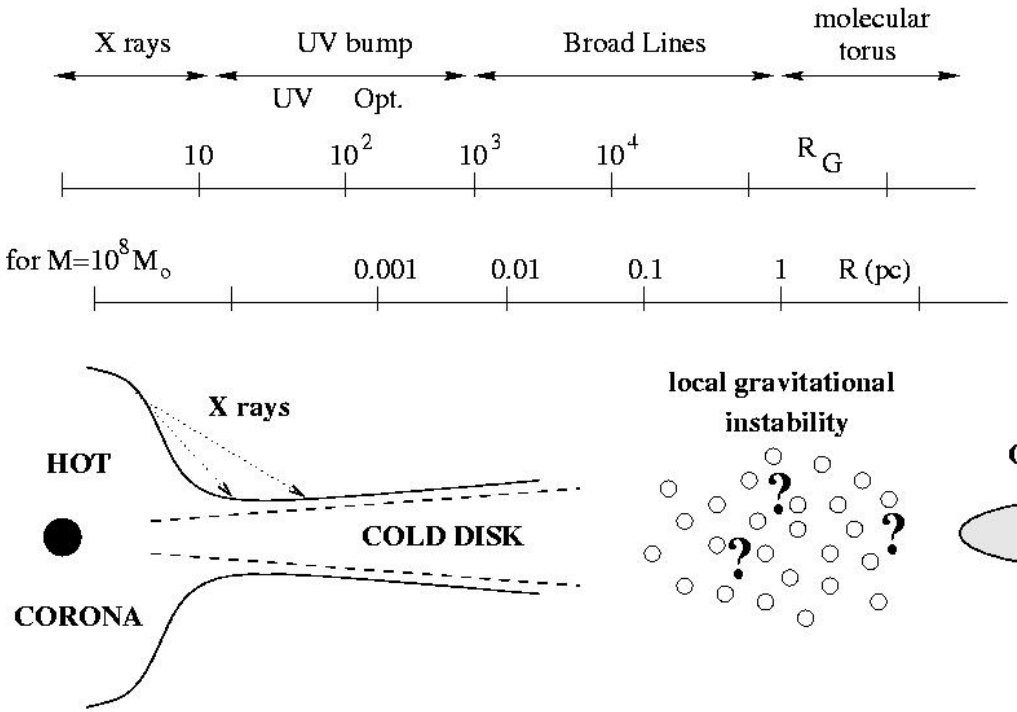

The extreme luminosities emitted by AGN

bolometric $L_{AGN} \approx 10^{44}$–10^{46} erg s^{-1}

made it clear that the easiest way to explain them was through the release of gravitational energy. In the mid-60s the concept of a supermassive black hole (**SMBH**) surrounded by a viscous disk of accreting matter gained popularity (Zeldovich & Novikov 1964, Lynden-Bell 1966), and has become the standard model for AGN, still used today.

(Collin 2001)

Basics of the BH paradigm: mass of the BH

In order to guarantee the stability of the system: $\vec{F}_{\rm rad} \le \vec{F}_{\rm grav}$

The radiation pressure is $P_{\rm rad} = \frac{f}{c} = \frac{L}{4\pi r^2 c}$, so that $\vec{F}_{\rm rad} = \sigma_e \frac{L}{4\pi r^2 c}\hat{r}$,

where σ_e is the Thompson cross-section.

This has to balance the gravity exerted over an electron-proton pair:

$$\vec{F}_{\rm grav} = -\frac{GM_\bullet (m_p + m_e)}{r^2}\hat{r}$$

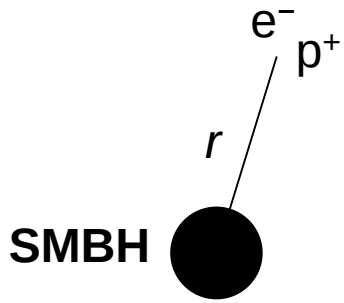

The condition $\left|\vec{F}_{\rm rad}\right| \le \left|\vec{F}_{\rm grav}\right|$ then implies that

$$L \le \frac{4\pi G c m_p}{\sigma_e} M_\bullet \approx 6.31\times10^4 M_\bullet \ {\rm erg\ s^{-1}} \approx 1.26\times10^{38}(M_\bullet / M_\odot) \ {\rm erg\ s^{-1}}$$

This is known as the Eddington limit, which can be used to establish a minimum for the mass of the BH:

$$M_{\rm E} = 8\times10^5 L_{44}\, M_\odot$$

For typical Seyfert galaxies $L \approx 10^{44}$ erg s^{-1} , so $M_{\rm Sy} \approx 8 \times 10^5\ M_\odot$

QSOs $L \approx 10^{46}$ erg s^{-1} , so $M_{\rm QSO} \approx 8 \times 10^7\ M_\odot$

The Eddington luminosity is the maximum luminosity

$$L_{\rm E} = \frac{4\pi G c m_p}{\sigma_e} M_\bullet$$

emitted by a body of mass $M_\bullet$ that is powered by spherical accretion.

Basics of the BH paradigm: rate of accretion

The process thought to power AGN is the conversion of mass to energy $E = \eta m c^2$ where η is the efficiency, that we want to evaluate. The rate at which the energy is emitted gives us the rate at which the energy must be supplied to the nucleus.

$$L = \dot{E} = \eta \dot{m} c^2$$

To power an AGN $\dot{M}_\bullet = \frac{L}{\eta c^2} \approx 1.8 \times 10^{-3} \frac{L_{44}}{\eta} \; M_\odot \; \mathrm{yr}^{-1}$

Lets estimate η now. The potential energy of a mass m is $U = GM_\bullet m / r$. The rate at which the infalling material can be converted into radiation is given by

$$L = \dot{U} = \frac{GM_\bullet}{r}\dot{m} = \frac{GM_\bullet \dot{M}_\bullet}{r} \quad \text{so} \quad \eta \propto M_\bullet / r$$

Ignoring relativistic effects, the energy available from a particle of mass m falling to $5R_S$, where R_S is the Schwarzschild radius of the BH ($R_S = 2GM_\bullet/c^2$), is

$$U = GM_\bullet m / 5R_S = 0.1 mc^2 \Rightarrow \eta = 0.1$$

For typical QSOs, $L \approx 10^{46}$ erg s^{-1}, so $\dot{M}_{QSO} \approx 2\, M_\odot$ yr^{-1}.

The Eddington accretion rate is the necessary accretion rate to sustain the Eddington luminosity:

$$\dot{M}_E = \frac{L_E}{\eta c^2} = 2.2 M_8 \; M_\odot \; \mathrm{yr}^{-1}$$

And the BH growth-time is

$$\tau_\bullet = \frac{\eta \sigma_e c}{4\pi G m_p} = 4 \times 10^7 (\eta / 0.1) \; \mathrm{yr}$$

Evidence for SMBHs in AGN: velocity fields

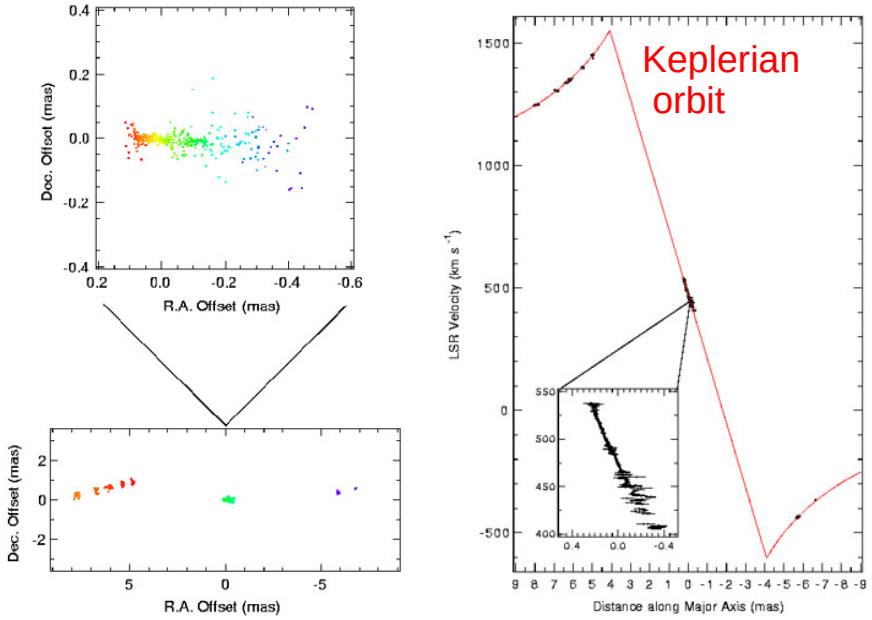

(Miyoshi et al. 1995)

H_2O megamaser @ 22 GHz detected in NGC 4258 in a warped annulus of 0.14 − 0.28pc and less than 10^{15} cm of thickness, with a beaming angle of 11° (Miyoshi et al. 1995, Maloney 2002): combining the Doppler velocities (±900km s^{-1}) and the time to transverse the angular distance (0.14 pc) gives the mass of the nucleus 3.9 x $10^7 M_\odot$ within $r \leq 0.012$ pc

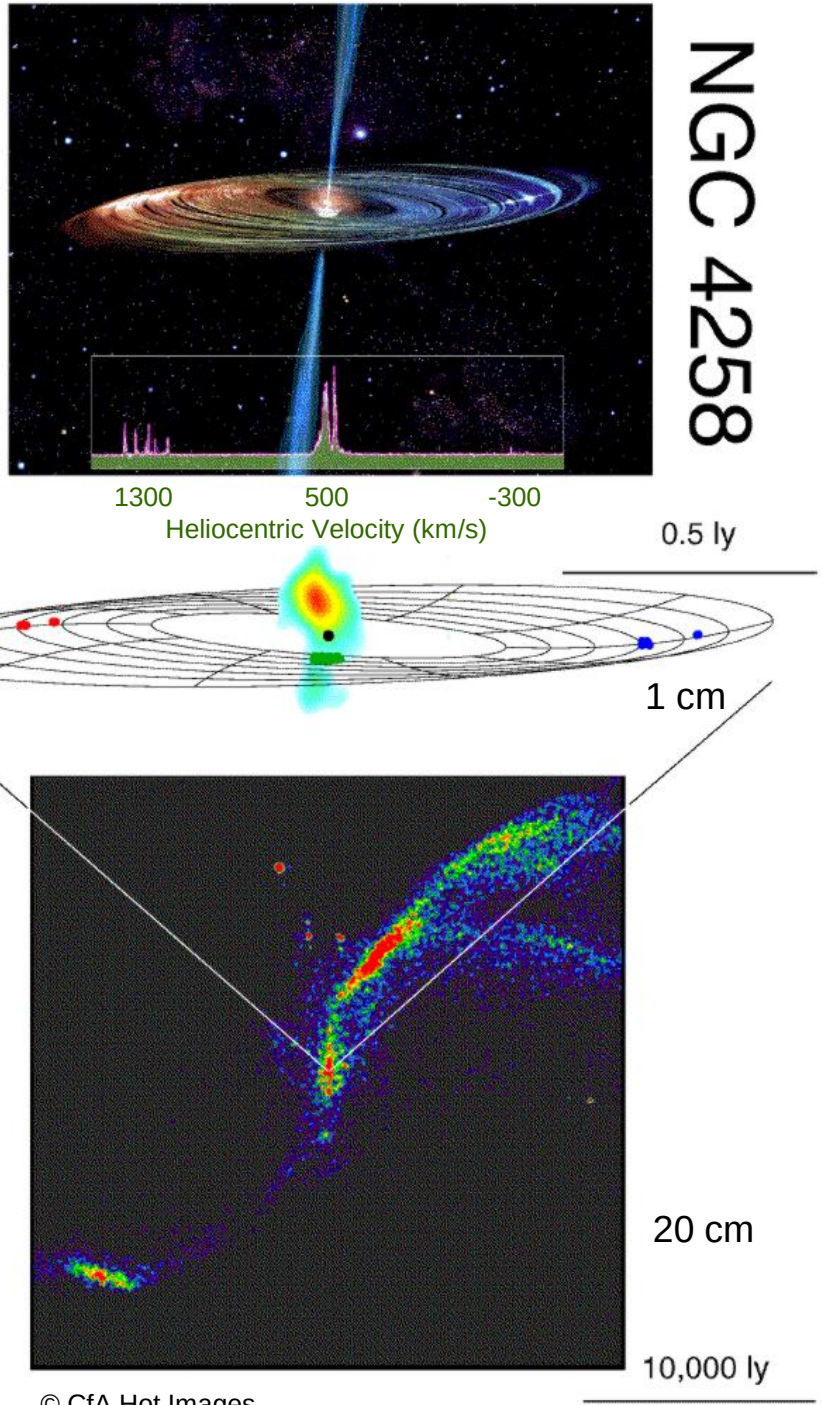

Evidence for SMBHs in AGN: velocity fields

Surveys of H_2O megamasers (Braatz, Wilson & Henkel 1997), with 354 AGN surveyed ($v \leq 7000$ km s^{-1}), show 16 sources, all in the nuclei of Sy 2s (10/141) and LINERs (5/67). There are no Sy 1 masers detected, probably because the masers are beamed towards the plane of the tori. Sy 2s with high N_H absorbing columns are more likely to create masers.

Another good case to measure the BH is NGC 1068 (Sy 2) with a 0.65pc – 1.1pc annulus and Doppler velocities of ±300 km s^{-1}, which implies a central mass of $1.5 \times 10^7 M_\odot$, but the calculation is uncertain by factors of a few since the orbit is sub-keplerian $v \propto R^{-0.31\pm0.02}$ (Greenhill et al. 1996).

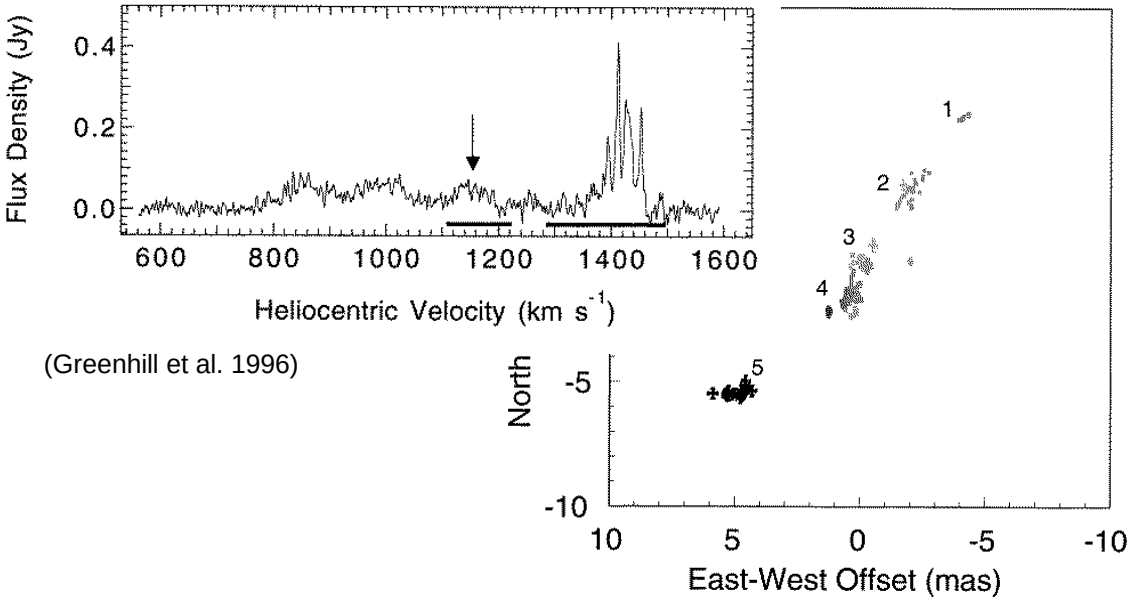

(Greenhill et al. 1996)

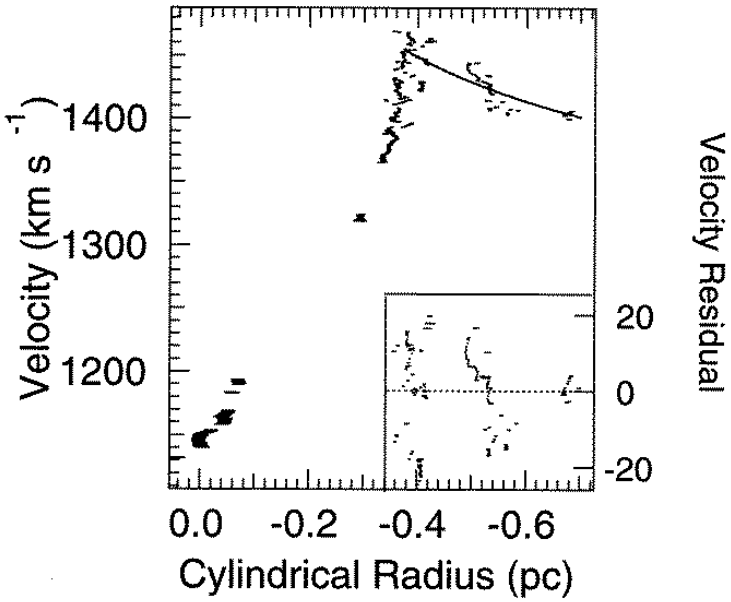

Evidence for SMBHs in AGN: Kα Fe line

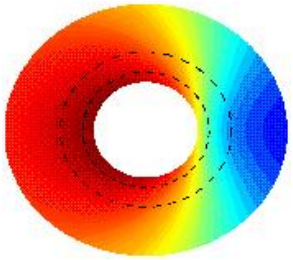

The iron line is clearly detected in the ASCA X-ray spectra of MGC–6–30–15 (Tanaka et al. 1995). The profile is skewed with an extended red wing due to gravitational redshift, and a prominent blue wing which is relativisticaly boosted due to the high orbital velocities of the disk.

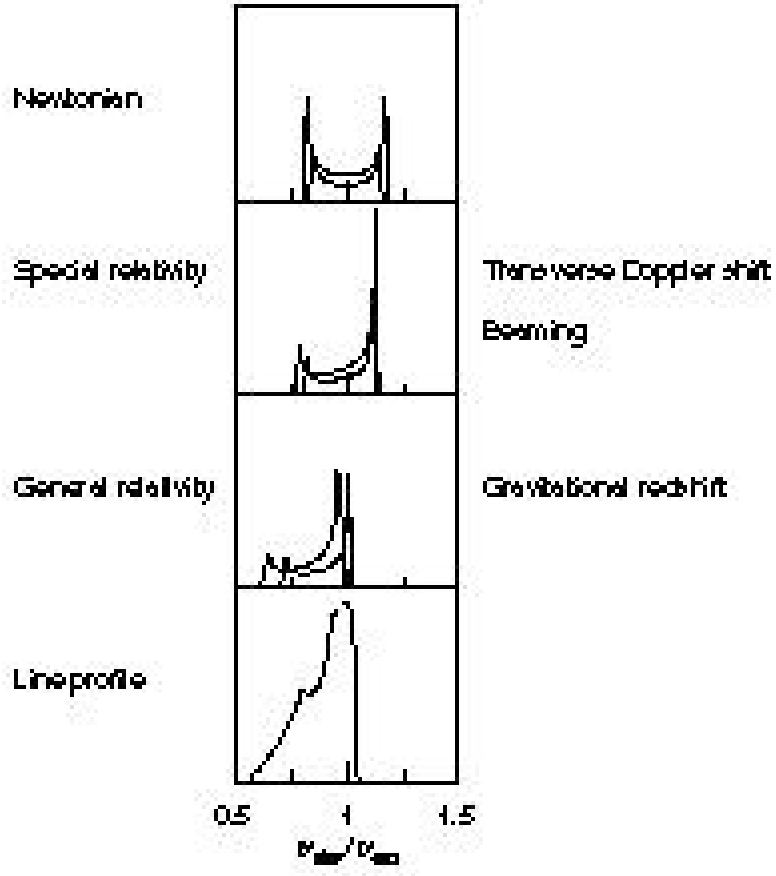

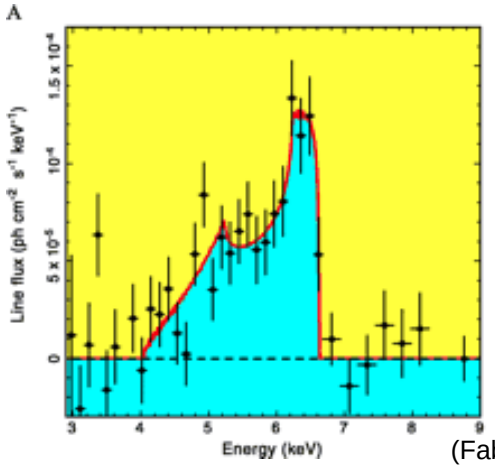

(Fabian 1999)

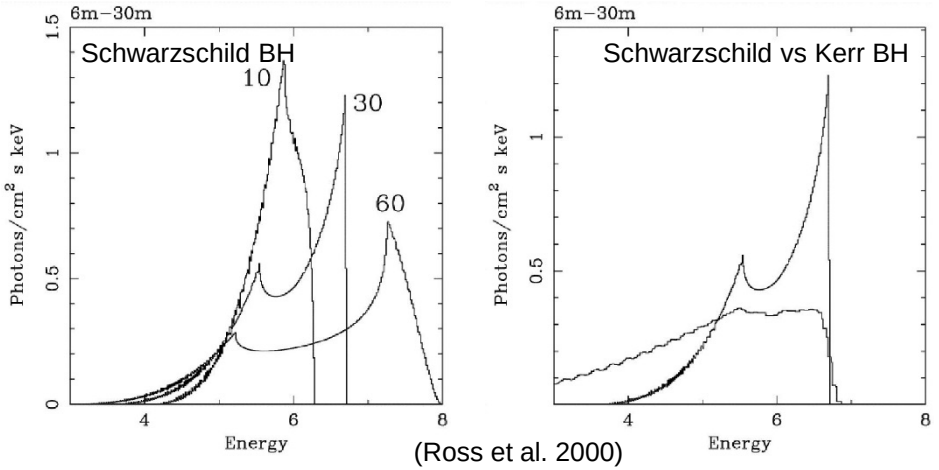

(Ross et al. 2000)

Evidence for SMBHs in AGN: Kα Fe line

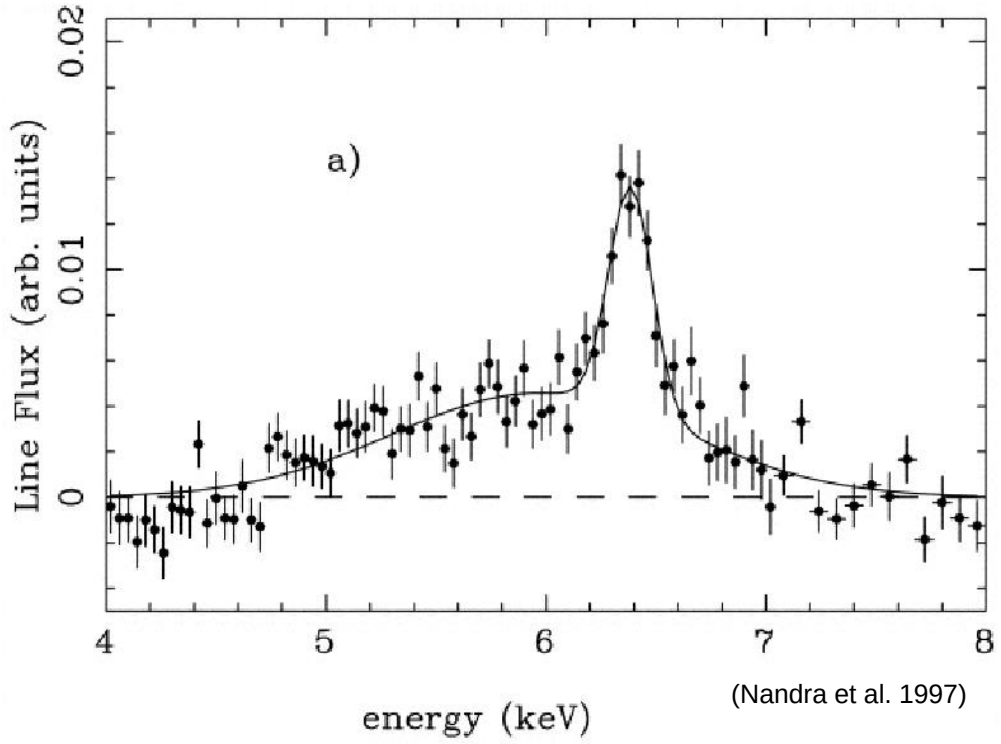

(Nandra et al. 1997)

Broad lines like those of MCG-6-30-15, once thought to be common in most Sy 1 and 2s (Nandra et al. 1997, Turner et al. 1997,) have not been confirmed by XMM/Chandra in such high percentages (Yaqoob 2007 for conciliatory remarks). A broad line is confirmed in another Sy 1 (Mrk 766), and narrow (σ<5000 km/s, EW~75 eV) Kα lines are found in most Sy 1s, but not in QSOs (e.g. 3C 273)! It is now believed that they could originate in molecular torus or outer BLR (Reeves et al. 2003).

Evidence for SMBHs in AGN: Kα Fe line

Not all iron lines are like MCG-6-30-15:- the Seyfert 1 NGC 5548

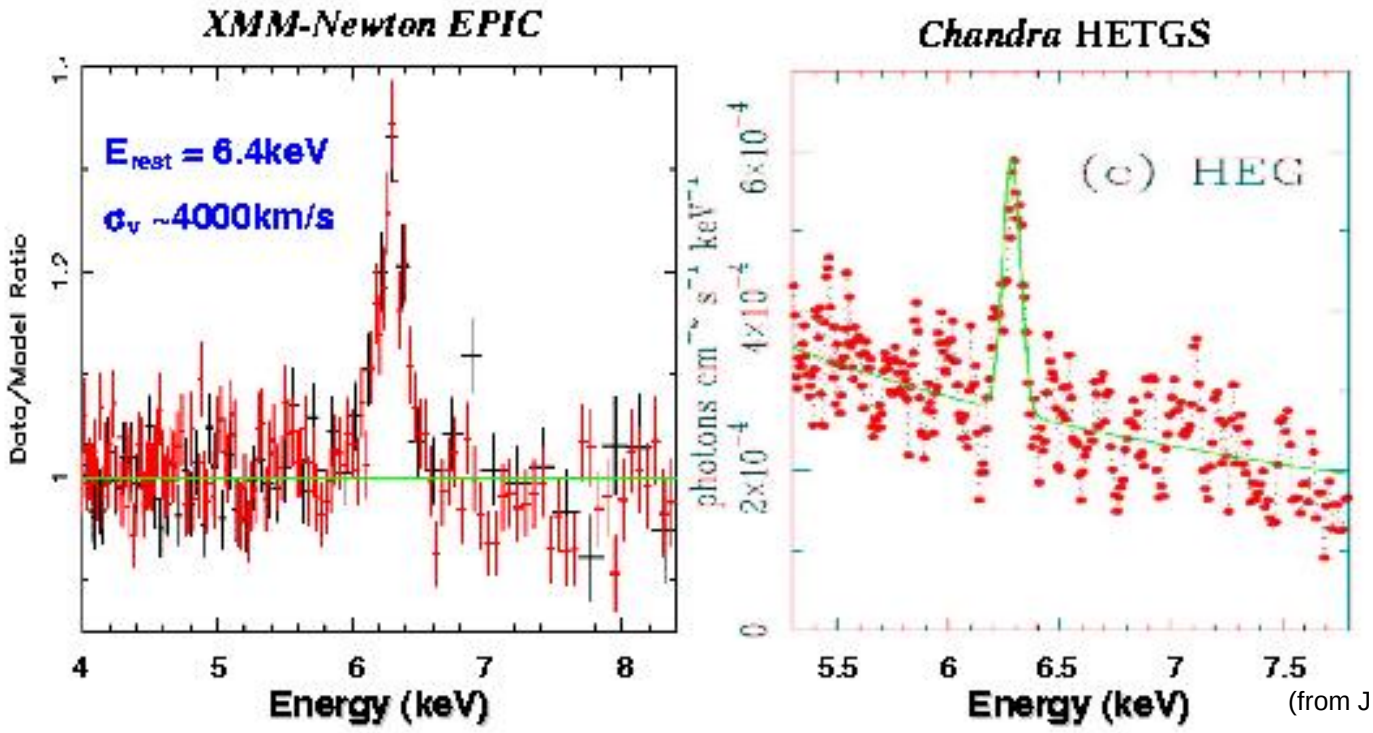

(from J. Reeves´ web page)

Broad lines like those of MCG-6-30-15, once thought to be common in most Sy 1 and 2s (Nandra et al. 1997, Turner et al. 1997,) have not been confirmed by XMM/Chandra in such high percentages (Yaqoob 2007 for conciliatory remarks). A broad line is confirmed in another Sy 1 (Mrk 766), and narrow (σ<5000 km/s, EW~75 eV) Kα lines are found in most Sy 1s, but not in QSOs (e.g. 3C 273)! It is now believed that they could originate in molecular torus or outer BLR (Reeves et al. 2003).

Weighing BHs in AGN : reverberation

The BLR is photoionized, since it responds to continuum variations, with a certain delay, which is a function of the BLR geometry, viewing angle, line emisivity, etc.

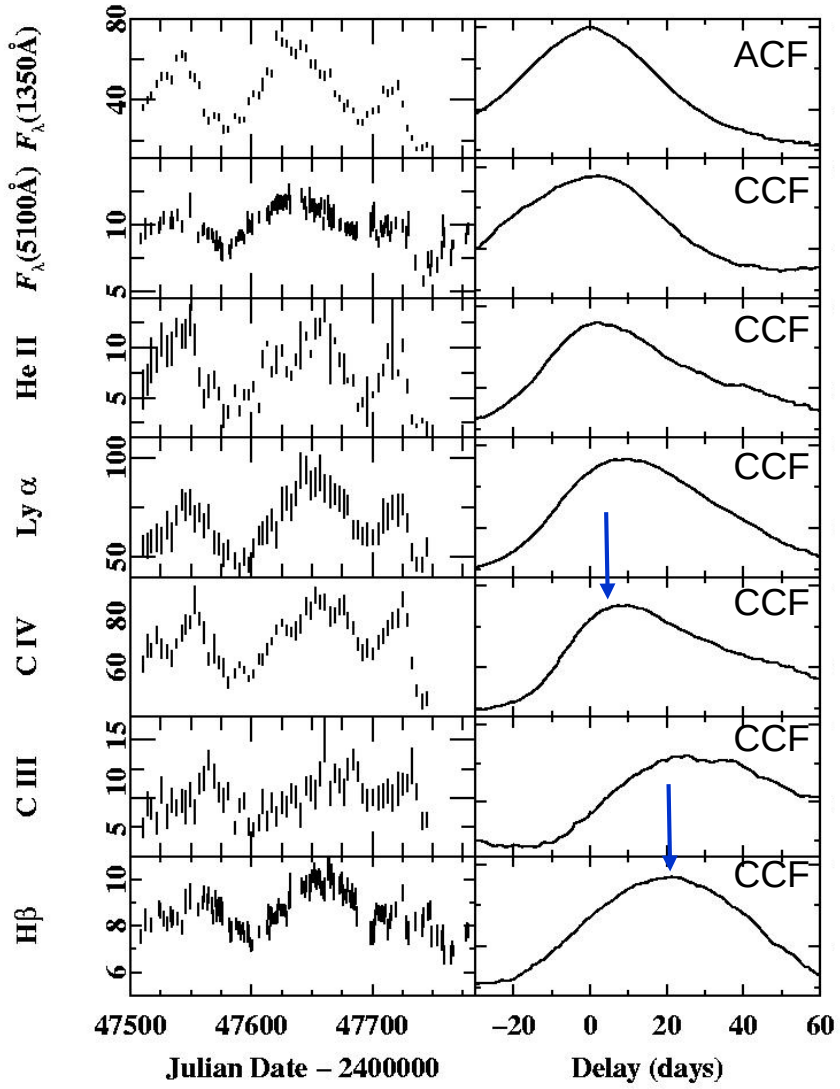

(Peterson 2001, data from Clavel et al. 1992, Peterson et al. 1992)

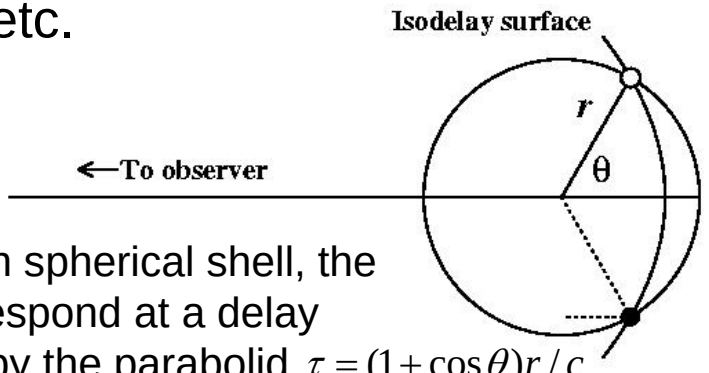

e.g., for a thin spherical shell, the BLR would respond at a delay time τ given by the parabolid $\tau = (1+\cos\theta)r/c$

In general the line response is given by

$$I(t) = \int \Psi(\tau) L(t-\tau) d\tau$$

where Ψ is called transfer function. The centroid of the cross-correlation function between the continuum and the line gives the mean radius of emission:

$$\mathrm{CCF}(\tau) = \int \Psi(\tau') \mathrm{ACF}(\tau - \tau') d\tau'$$

where ACF is the autocorrelation function of the continuum.

Weighing BHs in AGN: reverberation at high-*L*

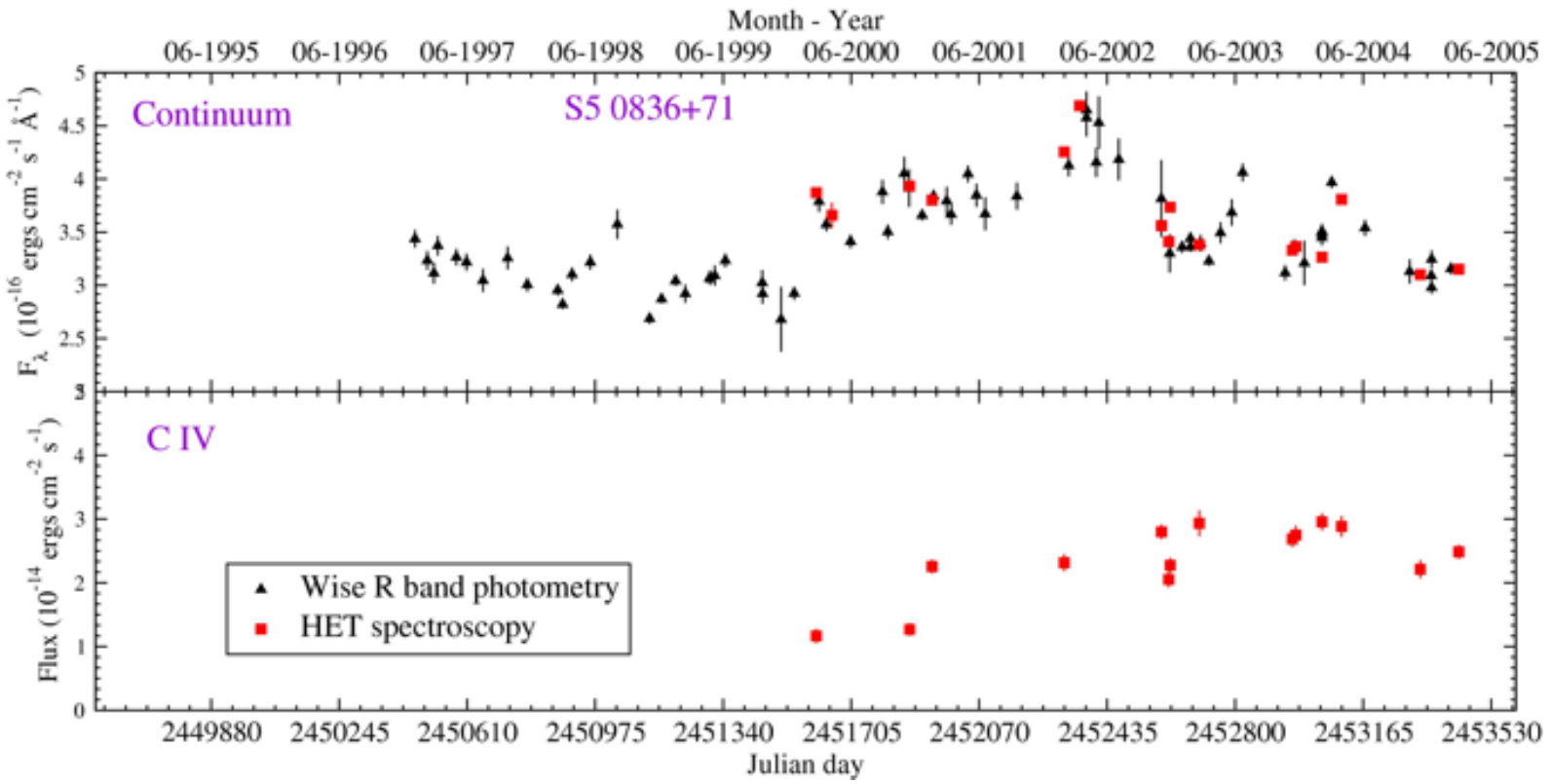

(Kaspi et al. 2006)

Difficulty to measure at high-*L* (program in 1-m Wise Obs., Kaspi et al. 2006):

$\lambda L_\lambda(5100\ \text{Å}) = 1.1\times10^{46}$ erg/s , $z = 2.172$

Rest frame time lag: 188^{+27}_{-37} days

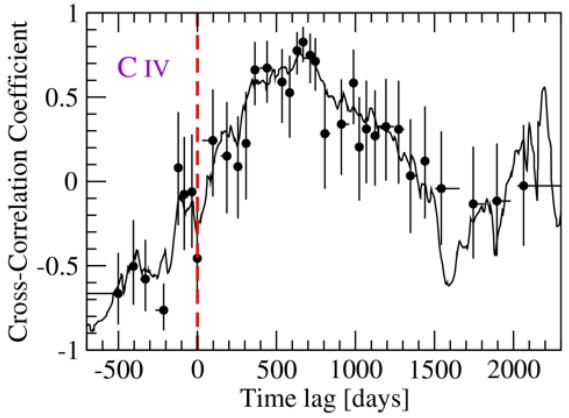

Weighing BHs in AGN : reverberation

If the kinematics of the BLR is keplerian, we can apply the virial theorem $\frac{GM_\bullet}{r_{\rm BLR}} = f\sigma^2$ with *f,* a factor close to 1. Measuring the line widths (FWHM) of the emission lines, we have an estimate of the velocity dispersion σ, and thus,

$$M_\bullet \approx (1.45\times10^5 M_\odot)\left(\frac{c\tau}{\rm lt-day}\right)\left(\frac{v_{\rm rms}}{10^3\,{\rm km\,s^{-1}}}\right)^2$$ (Wandel, Peterson & Malkan 1999)

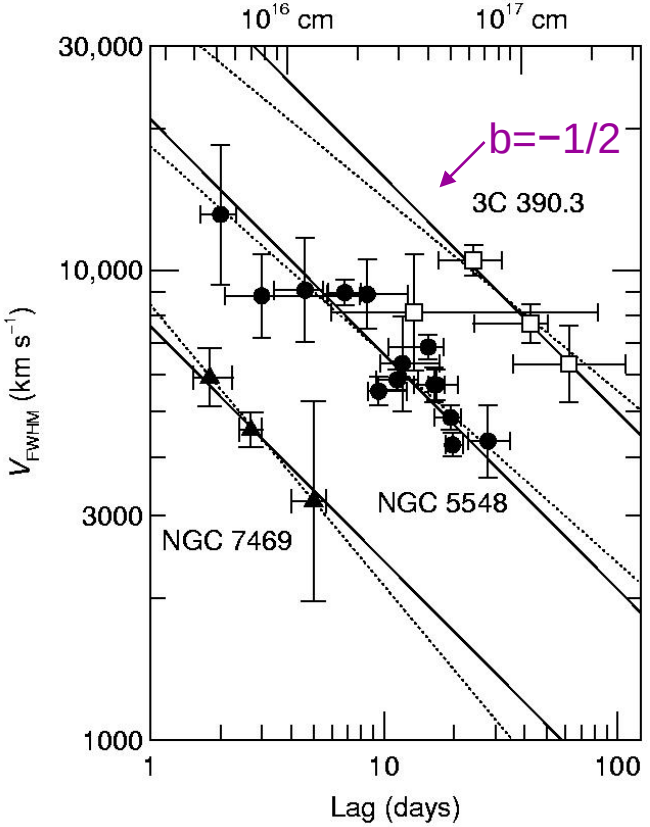

(Peterson & Wandel 2000)

Different lines give you the same answer, even if the $r_{\rm BLR}$ measured is different.

$$\log v_{\rm FWHM} = a + b\log c\tau$$

The masses derived by this method range from $M = 10^7\,M_\odot$ for Sy 1s (i.e., in the range of the LINER NGC 4258) to $M = 10^9\,M_\odot$ for QSOs.

Weighing BHs in AGN: photoionization masses

The mass can also be estimated using solely photoionization calculations.

The number of photons emitted by the central source per second that can ionize H is given by $Q_{\rm ion} = \int_{\nu_0}^{\infty} \frac{L_\nu}{h\nu} d\nu$. The ionization parameter *U* is defined as the ratio of the photon number density to the particle density.

$$U \equiv \frac{Q_{\rm ion}}{4\pi r^2 c n_{\rm e}}$$

A straightforward prediction of the photoionization calculation is that if *U* and n_e are similar in AGN, then $r_{\rm BLR} \propto L^{1/2}$, which is actually observed. *U* and n_e are constrained by photoionization models that can reproduce the emission-line ratios: $U = 0.1 - 1$ and $n_e = 10^{10} - 10^{11}$ cm^{-3} (Rees, Netzer & Ferland 1989). Invoking keplerian orbits again:

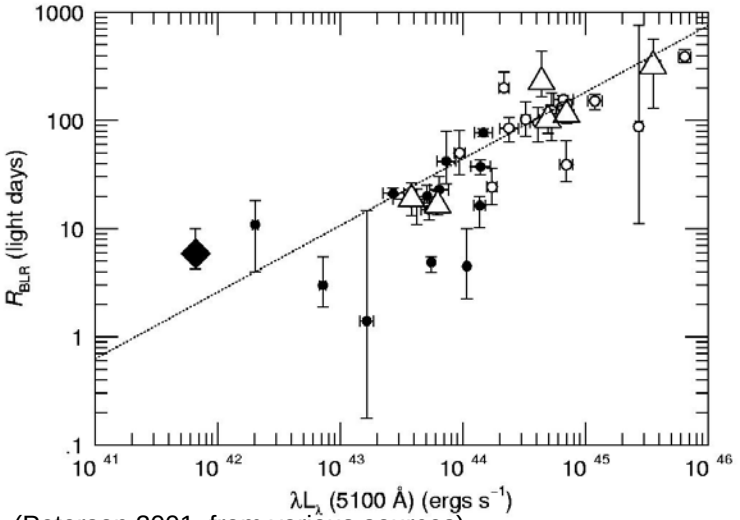

(Peterson 2001, from various sources)

$$M_\bullet \approx \frac{r_{\rm BLR} v^2}{G} = K \left(\frac{L_{\rm ion}}{U n_e E_{\rm ion}} \right)^2 v_{\rm FWHM}^2 \quad , \quad \text{where } K = \frac{3}{4} \frac{1}{G\sqrt{4\pi c}}$$

The two methods have been compared in a sample of 17 Sy 1s and 2 QSOs (Wandel et al. 1999), and the agreement is reasonably good, but photoionization masses are slightly underestimated.

Weighing BHs in AGN: reverberation masses

Reverberation sizes measured for 36 AGN show a $R \propto L^{\alpha}$ with α= 0.5-0.7 (Peterson et al. 2005, Bentz et al. 2006, Kaspi et al. 2007), depending on the wavelength regime, regression method, and stellar line removal.

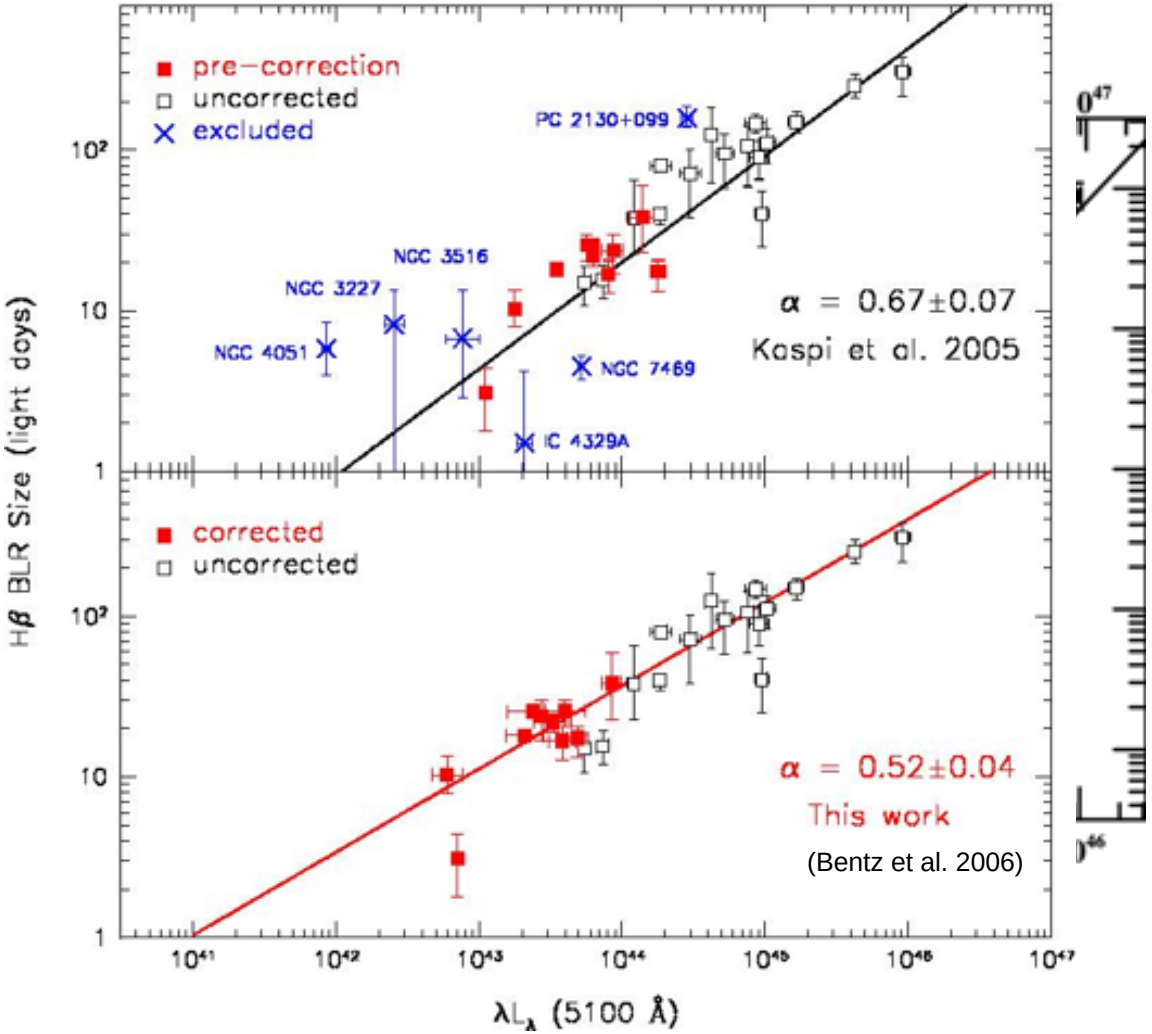

(Bentz et al. 2006)

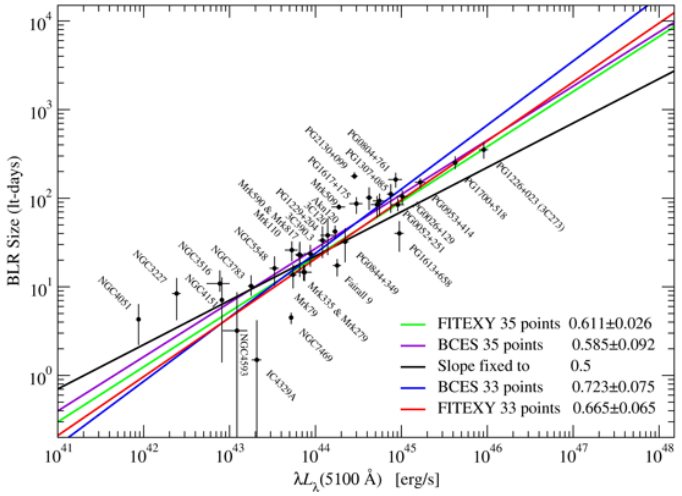

(Kaspi 2006)

Weighing BHs in AGN: line widths

Having established a $r \propto L^{\alpha}$ relationship and having calibrated it, *L* and *v* can give you the mass directly. Methods based just on line-widths and luminosity: Hβ (Wandel et al. 1999), Mg II (McLure & Jarvis 2002), C-IV (Vestergaard 2004) and compilation (Vestergaard & Peterson 2006):

$$\log M_{\bullet} = a \log\left[v^2 L^{\alpha}\right] + c$$

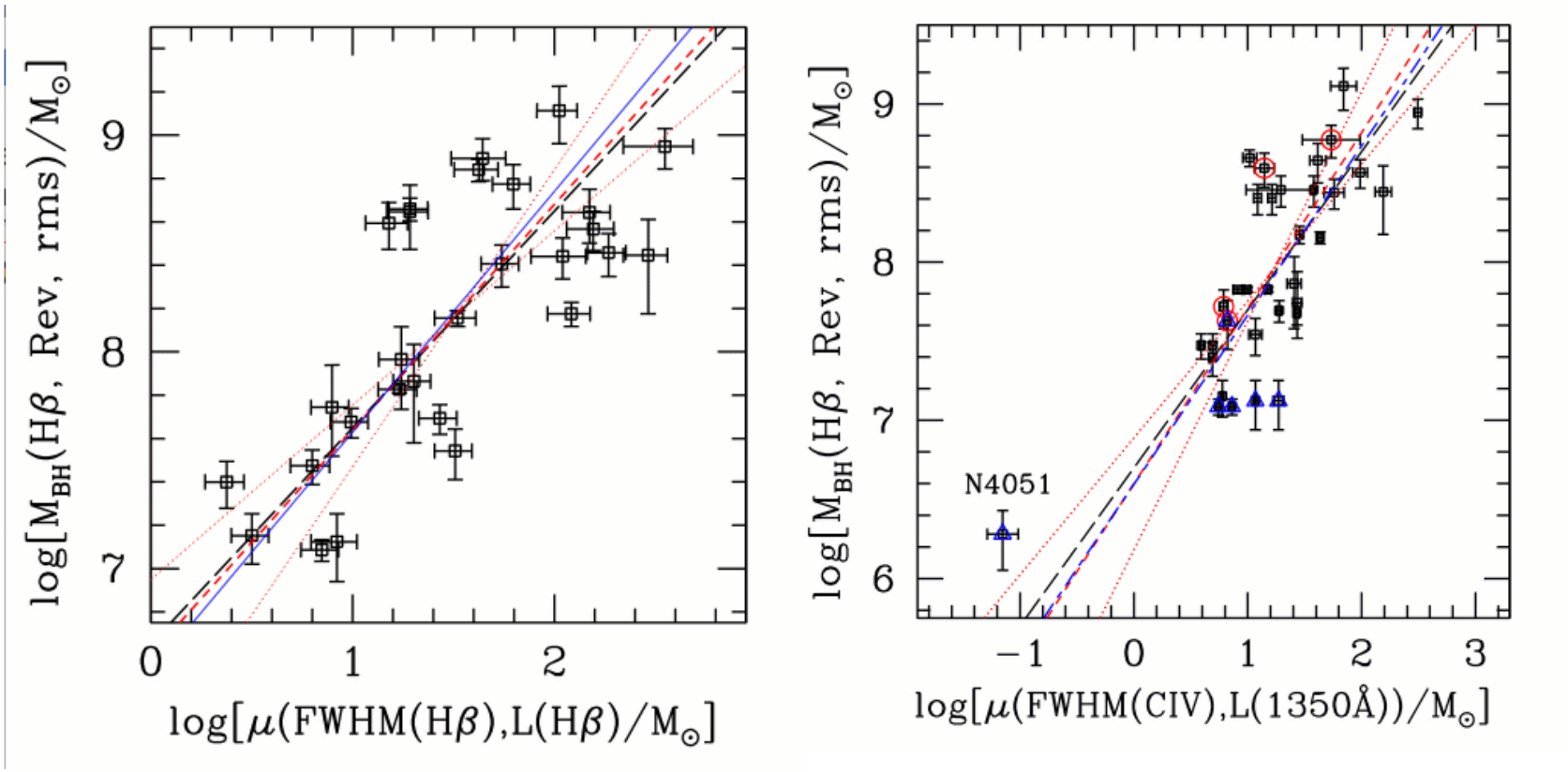

(Vestergaard & Peterson 2006)

AGN variability: extinction

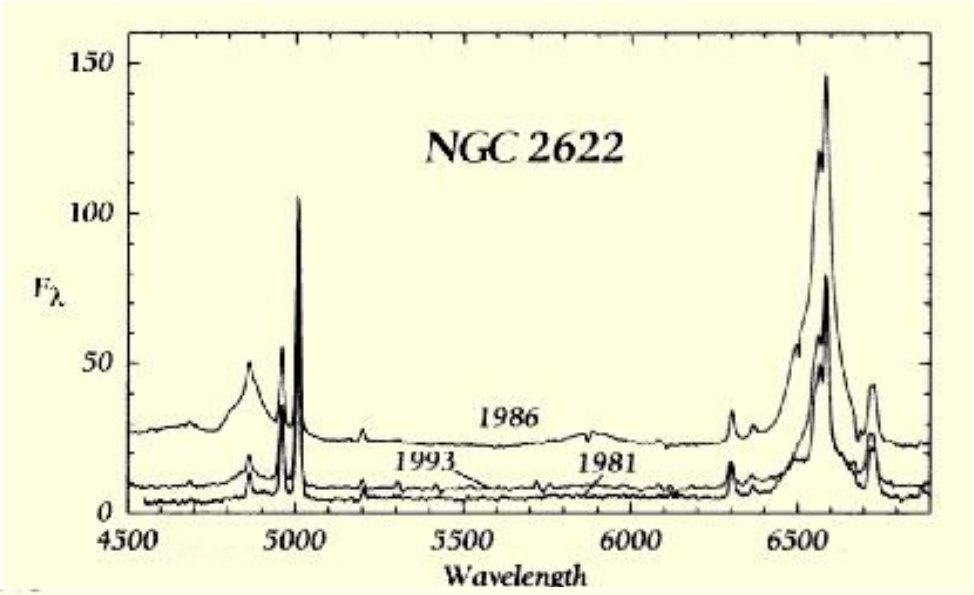

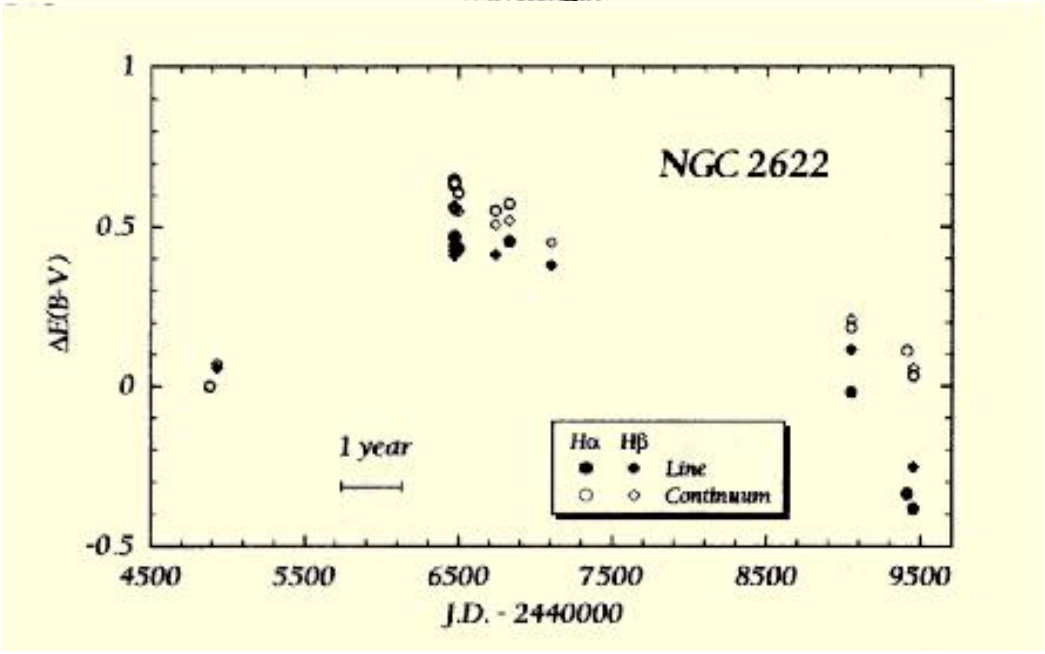

But beware that not all variations are necessarily due to intrinsic variability and its light-travel delays.

The variations in NGC 2622 are consistent with a reddening change obeying a local extinction curve. These variations could be due to a varying column of obscuration in our line of sight.

Hα/Hβ ≈ 10 in the Sy 1.8 stage, and it decreases as the flux increases. This is a clear indication of a change in reddening (Goodrich 1995).

AGN demographics: surveys

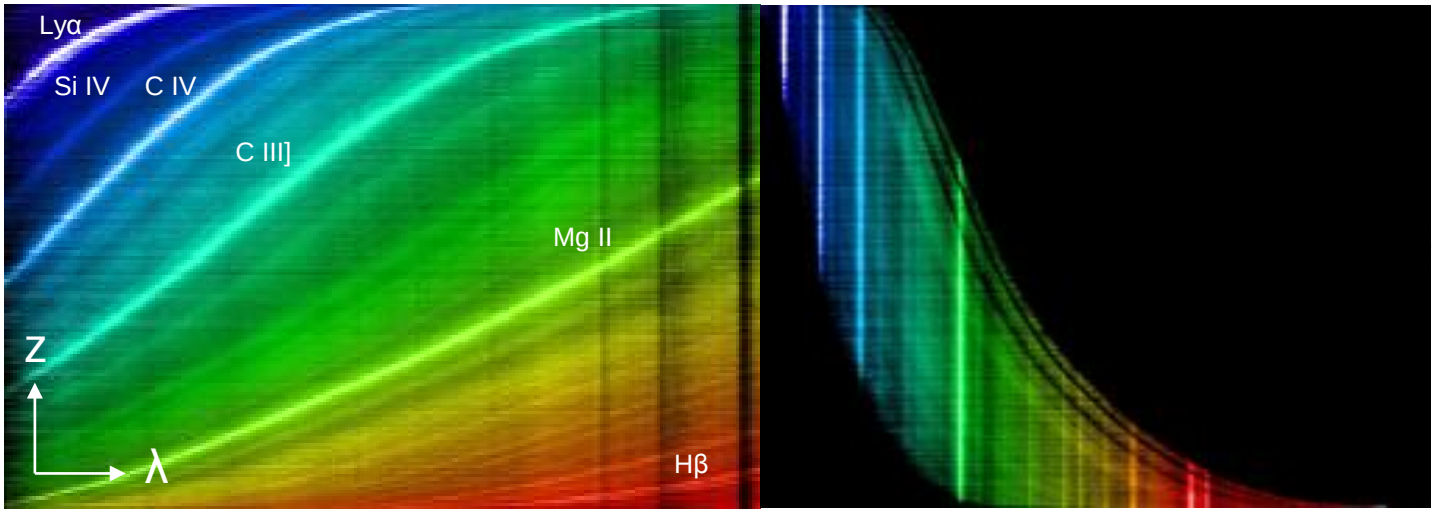

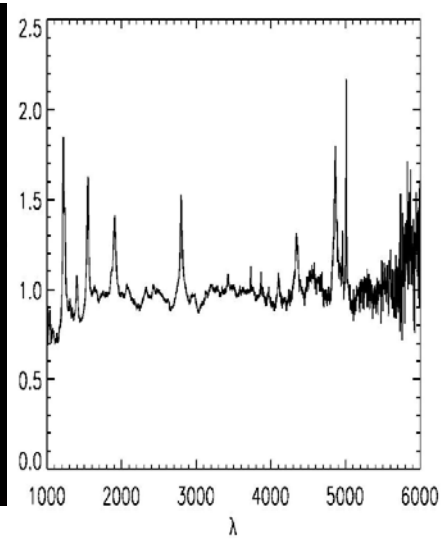

(2QZ web page, P. Francis´ web page)

Types of optical surveys:

- **Ultraviolet excess (UVX):** the optical region can be approximated by a power law $F(\nu) \propto \nu^{-\alpha}$, with $0.5 \leq \alpha \leq 0.5$, and this implies a colour $-0.8 \leq U - B \leq -0.7$. Good for QSOs at $z \leq 2.2$ The stellar-like contaminants are mainly white dwarfs. Example: Palomar Bright Quasar Survey.
- **Multicolour:** increases the probability that the candidates are real QSOs. They are also sensitive to QSOs at higher redshifts. Example: 2QZ, SDSS.
- **Slitless spectroscopy:** detects strong emission lines in photographic plates with an objective prism. Sensitive to QSOs $1.8 \leq z \leq 3.3$. Beset with selection effects which leads to incompletnesses. Examples: Large Bright Quasar Survey.
- **Variability:** detects variable star-like objects in a series of photographic plates taken over a few years. Not all QSOs are variable (luminosity-variability anti-correlation): it is incomplete in the high-luminosity end, at high-redshifts. Examples: Mike Hawkins.

AGN demographics: colour selection surveys

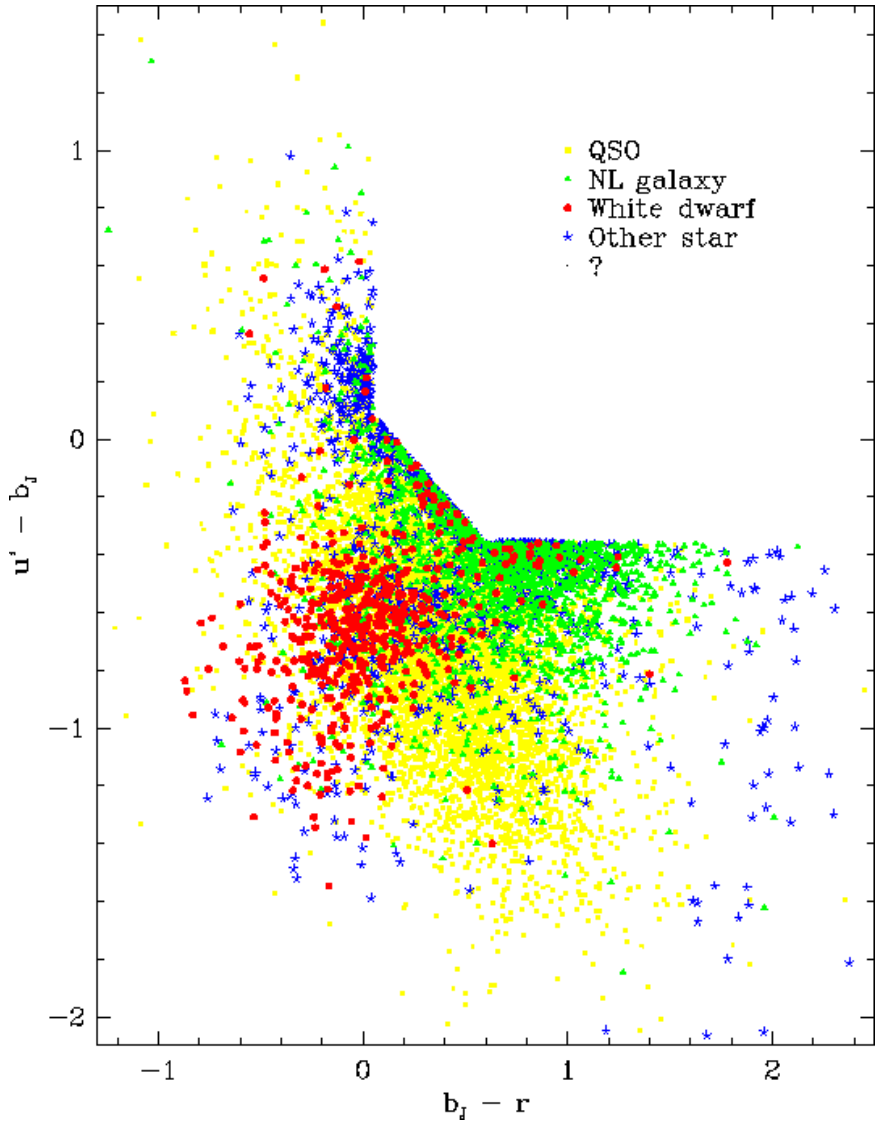

(2QZ web page)

QSOs:

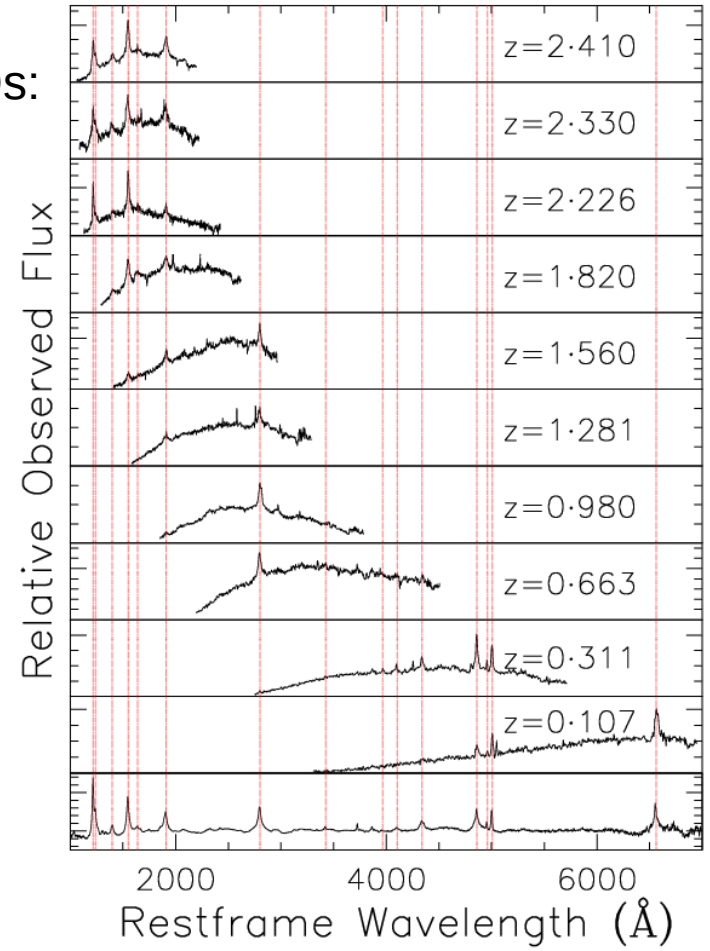

Other selected objects: NLGs And WDs

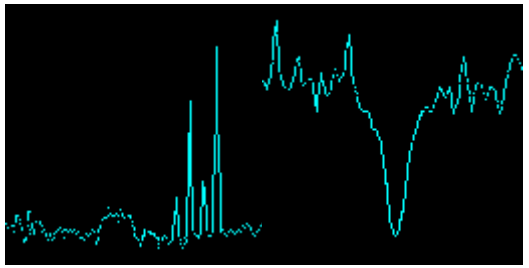

AGN demographics: luminosity function

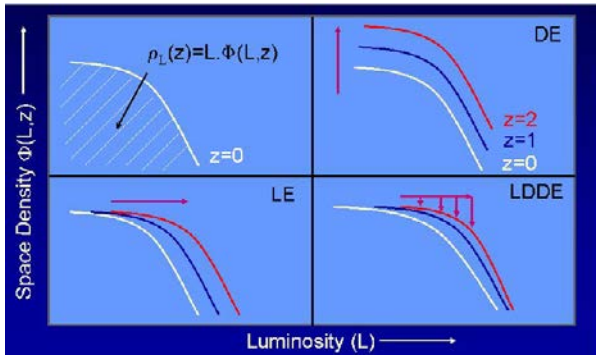

(Boyle 2001)

The luminosity function is a measure of the comoving space density of QSOs as a function of luminosity and redshift:

$$\Phi(L,z) \equiv \frac{d^2N(L,z)}{d\log L dV}$$

For QSOs it is usually parametrized as a double power-law

$$\Phi(L,z) = \frac{\Phi_*}{\left[\left(\frac{L}{L_*(z)}\right)^{\alpha} + \left(\frac{L}{L_*(z)}\right)^{\beta}\right]}$$

with 4 parameters: L_* , Φ_* , α, β

The LF at different redshifts shows that the QSO population experiences a strong cosmological evolution, which can be described as pure luminosity evolution

(Boyle et al. 1988...)

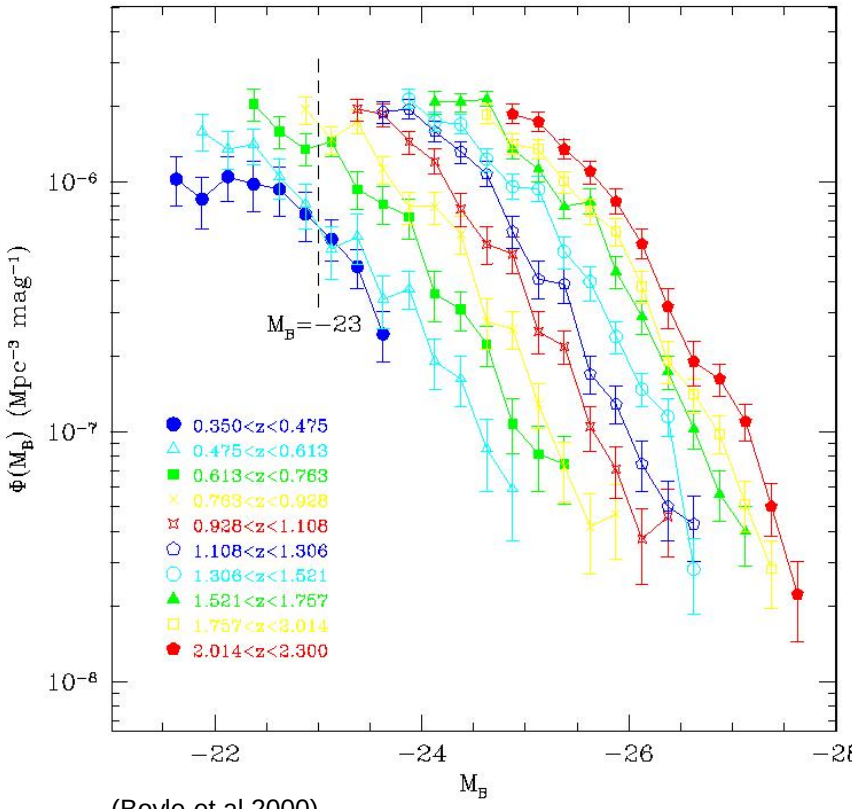

(Boyle et al 2000)

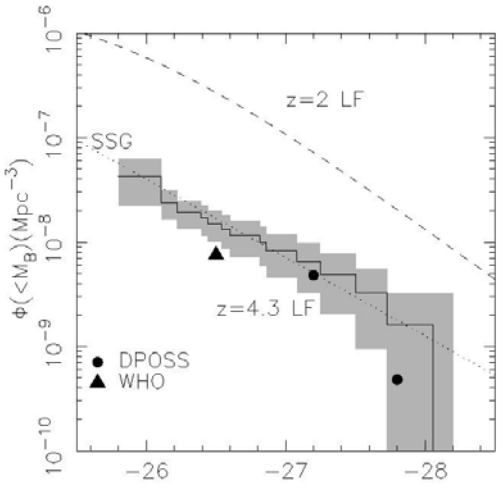

(Fan et al 2001)

AGN demographics: luminosity function

Table 4. QSO Luminosity Function: parameters ($\Omega_m = 1$)

$$\Phi(L,z) = \frac{d^2N}{d\log L dz} = \frac{\Phi^*}{\left[\left(\frac{L}{L^*(z)}\right)^{\alpha-1} + \left(\frac{L}{L^*(z)}\right)^{\beta-1}\right]}$$

	α	β	νL^* (W)	Φ^* ($d\log L^{-1}\mathrm{Mpc}^{-3}$)
Optical (4400Å)[27]	3.4	1.6	2.0×10^{37}	2.7×10^{-6}
Radio (2.7GHz)[46]	3.0	1.8	4.9×10^{34}	7.1×10^{-9}
X-ray (1keV)[119]	3.3	1.4	2.8×10^{38}	4.0×10^{-6}

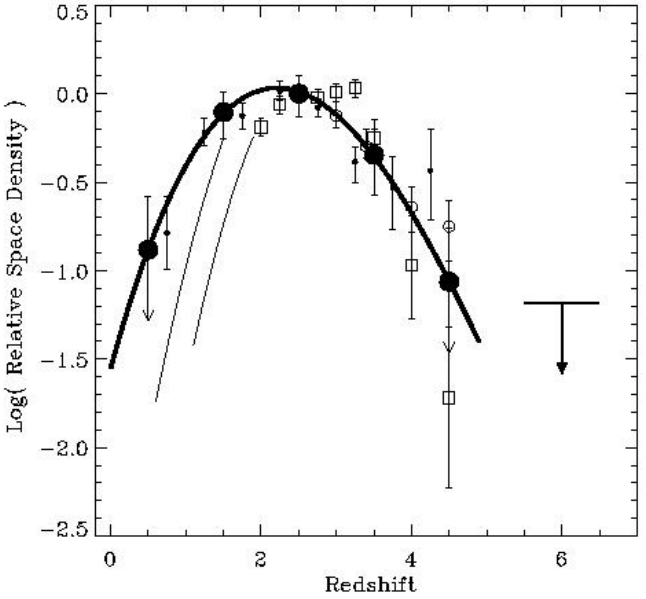

(Shaver et al. 1999)

Table 5. QSO Luminosity Function: evolution ($\Omega_m = 1$)

(Boyle 2001)

	Evolution	
Regime	$z < 2$	$z > 3$
Optical (680THz)[27,53]	$L^*(z) \propto 10^{1.40z-0.27z^2}$	$\Phi(z) \sim \Phi(3)3^{3-z}$
Radio (2.7GHz)[46,146]	$L^*(z) \propto 10^{1.18z-0.28z^2}$	$\Phi(z) \sim \Phi(2.5)5^{2.5-z}$
X-ray (240PHz)[119]	$L^*(z) \propto (1+z)^3$	$\Phi(L,z) \sim$ constant

The evolution of the LF shows that the QSO comoving density peaks at $z \approx 2.5$, which is often referred to as the quasar-epoch. The density experiences a strong decline thereafter. This decline is observed in both optical and radio surveys (Shaver et al. 1999).

QSO remnants: SMBHs in the local Universe

From the luminosity function of QSOs one can calculate the density of dead-QSOs in the local Universe (Sotlan 1982, ..., Ferrarese & Ford 2007), taking into account that the accretion rate is given by $\dot{M} = \frac{K_{\rm bol} L}{\eta c^2}$ where $K_{\rm bol}$ is the bolometric correction to the observed luminosity

$$\rho_{\rm dead\text{-}BH}(>M) = \frac{K_{\rm bol}}{\eta c^2} \int_0^\infty \int_L^\infty \frac{L'\Phi(L',z)}{H_0(1+z)\sqrt{\Omega_{\rm M}(1+z)^3+\Omega_\Lambda}} dL'dz$$

For $\Omega_{\rm M}$=1-0.3, Ω_Λ=0-0.7, H_0=70 km s^{-1}Mpc^{-1}, η~0.1, and an appropriate $K_{\rm bol}$ derived from AGN SEDs, the cumulative BH density mass due to accretion onto 0.3<z<5 is (1 − 4) x 10^5 $M_\odot$ Mpc^{-3}.

The local density of BHs in AGN can be calculated from the Sy 1 density and the photoionization masses (corrected to match reverberation), which turns out to be 5000 $M_\odot$ Mpc^{-3} ➡ the bulk of the mass connected to accretion from past QSO events does not reside in local AGN (Padovani et al. 1990).

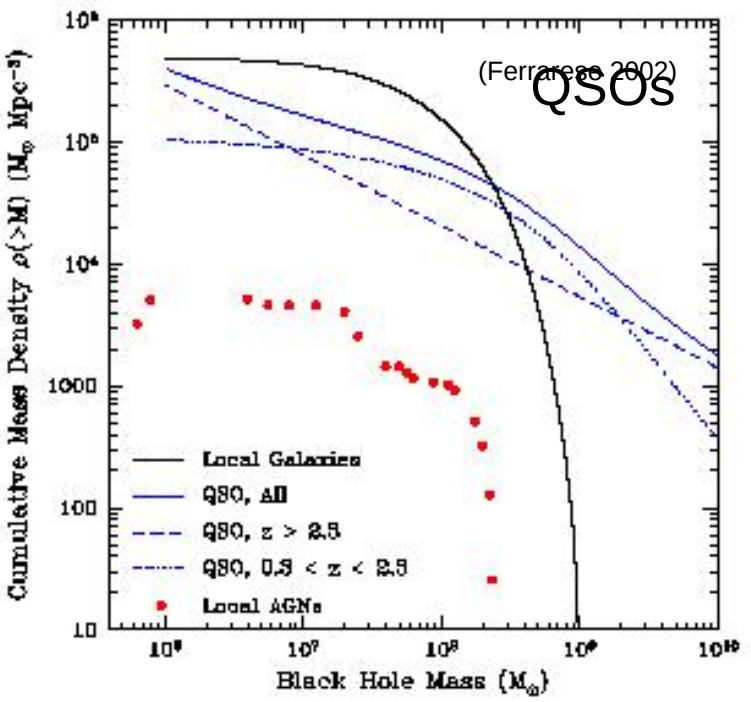

QSO remnants: SMBHs in the local Universe

The BH mass buried in quiescent galaxies can be estimated through the Magorrian relationship between BH mass and bulge luminosity.

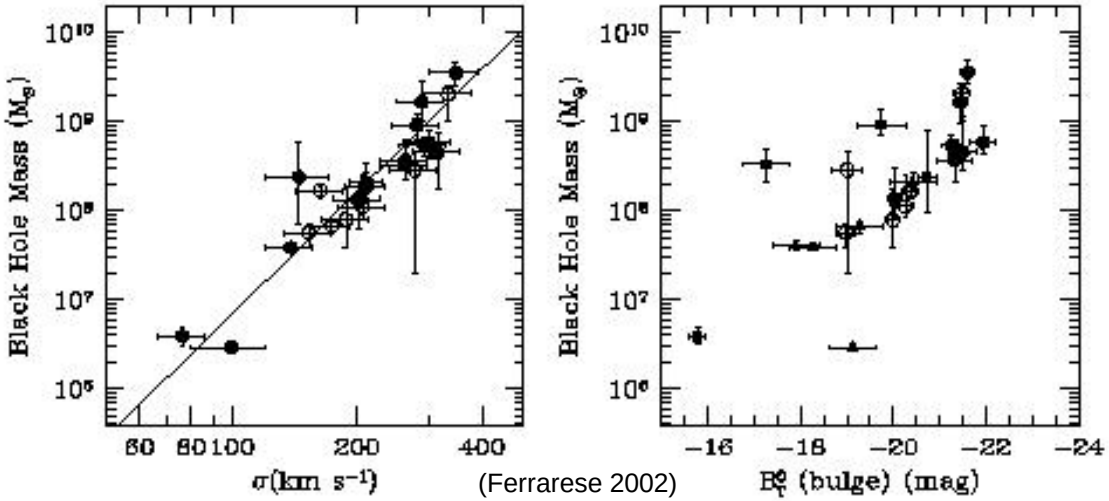

(Ferrarese 2002)

$$M_\bullet \approx 1.2\times10^8 M_\odot \left(\frac{\sigma}{200\text{km s}^{-1}}\right)^{3.75}$$

(Gebhardt 2000, Ferrarese & Merrit 2000)

$$\log M_\bullet = -0.36 M_B + 1.2$$

(Magorrian et al. 1998, Ferrarese & Merrit 2000)

Disregarding possible morphological type differences, the LF of local E/S0 $\Phi(L)dL = \Phi_0 (L/L_*)^\alpha \exp(-L/L_*) dL/L_*$ can be transformed into the local SMBH density through the Magorrian relationship, in general terms $L = AM_*^k$

$$\Psi(M_\bullet)dM_\bullet = \Psi_0 (M_\bullet/M_*)^{k(\alpha+1)-1} \exp\left(-(M_\bullet/M_*)^k\right) dM_\bullet/M_*$$

adopting a bulge-luminosity to galaxy-luminosity ratio. The mass density of SMBHs in local galaxies is (4 − 5) x 10^5 $M_\odot$ Mpc^{-3} .

This implies that all giant galaxies have probably experienced a QSO phase in the past (Wotjer 1955, ... Ferrarese 2002).

Low-*z* QSOs: host properties

If low-L AGN have a dichotomy between RL and RQ AGN host galaxies:

RQ tend to reside in early-type S gals

RL tend to reside in E gals

while SBs tend to reside in late-type S gals (e.g. Heckman 1985)

Luminous (M<-24, z<0.4) QSO hosts (both RL & RQ) reside in E gals $L \geq 2L_*$ with ~10 kpc scalelengths (Dunlop et al. 1993, Disney et al. 1995, Taylor et al. 1996, Hopper et al. 1997, McLure et al. 1999 —contested by Lewave et al. 2007), and follow the K-z relation of RGs.

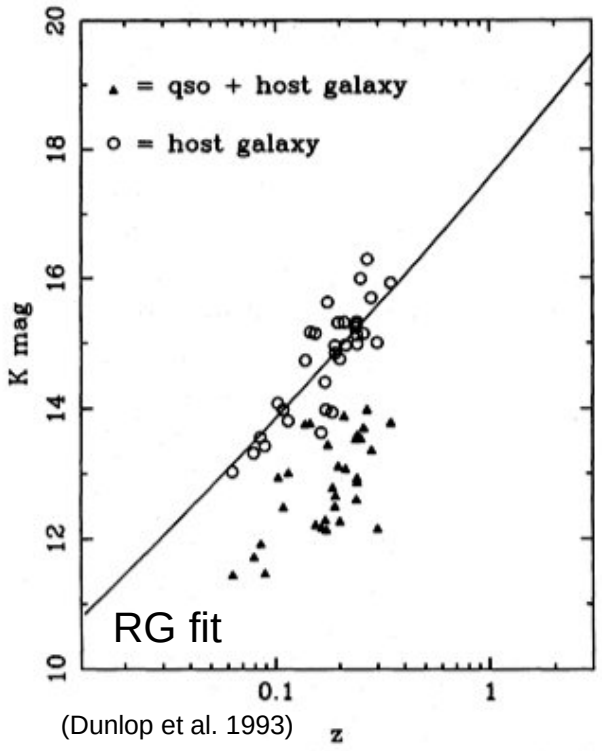

(Dunlop et al. 1993)

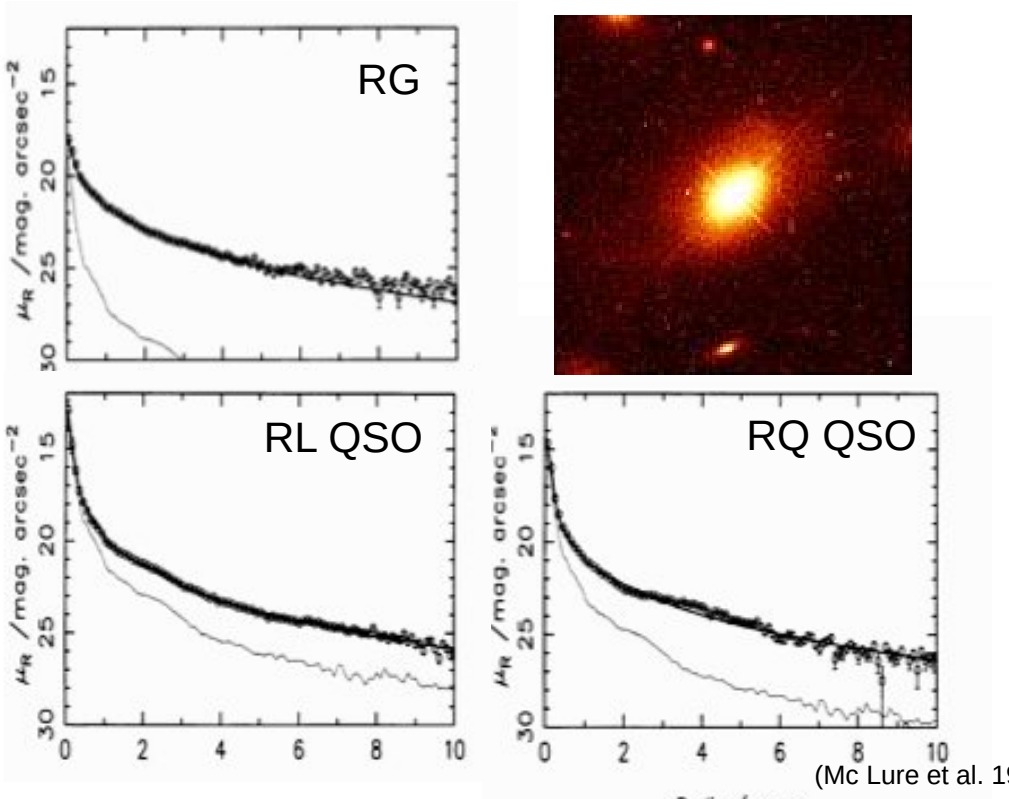

(Mc Lure et al. 1999)

QSO hosts at low-*z*: relics of past star formation?

Off-nuclear spectroscopy (Hughes et al. 2000, as per Boronson et al. 1985) of 26 AGN at $0.1 \leq z \leq 0.3$ shows the stellar features of an 8−12 Gyr population, but it may include a small (0−2% *M*) post-starburst contamination (Nolan et al. 2001). Because of the low S/N data, however, this result requires confirmation.

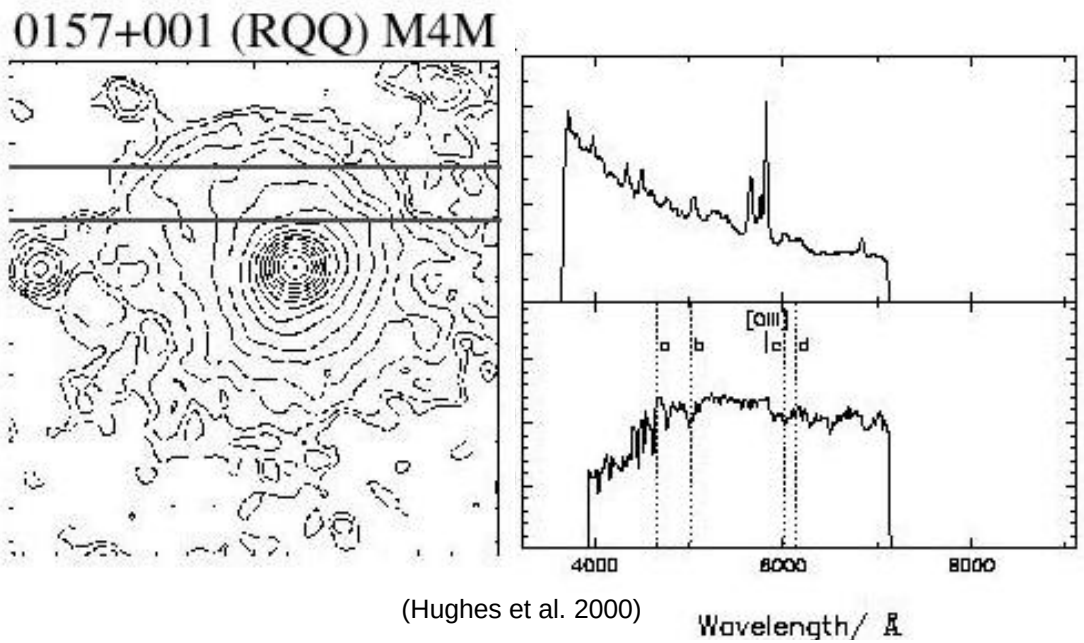

(Hughes et al. 2000)

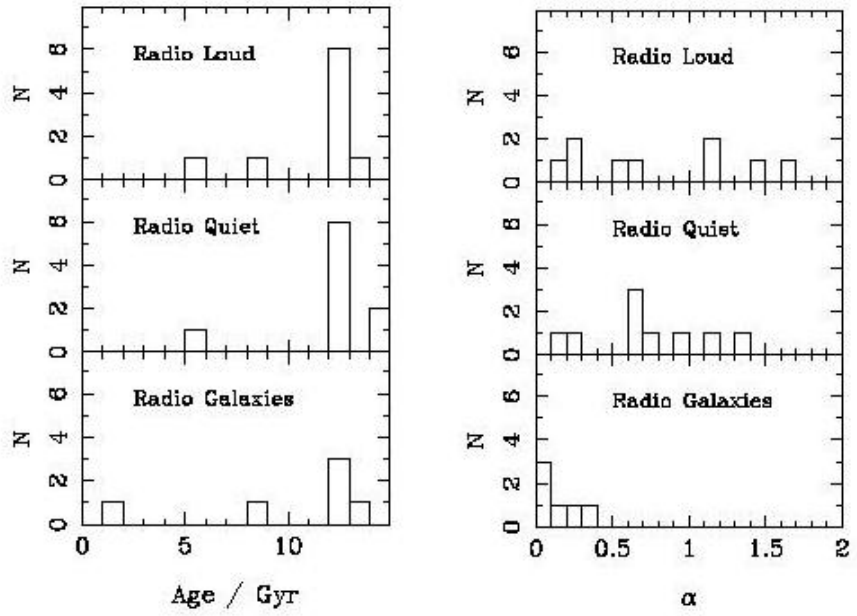

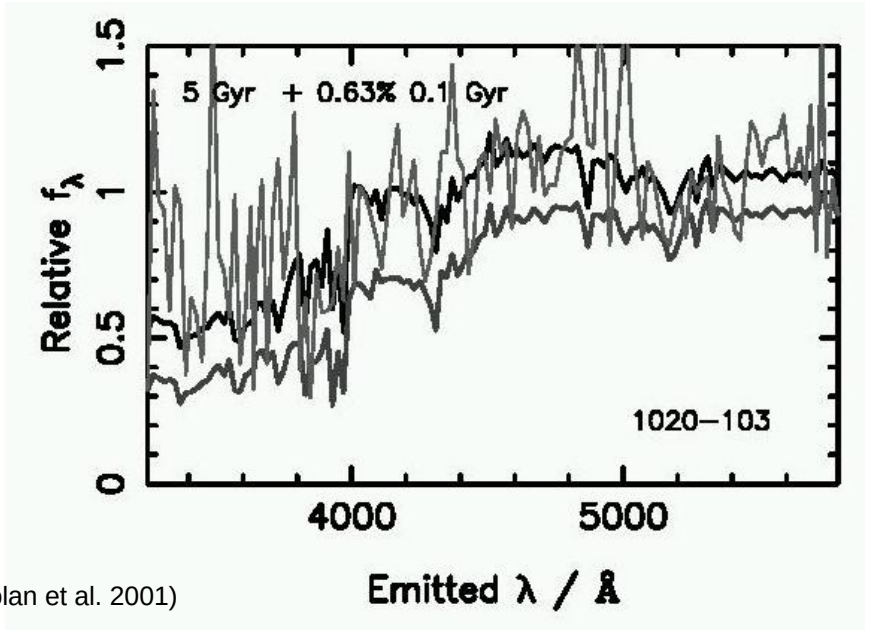

(Nolan et al. 2001)

QSO hosts at low-*z*: relics of past star formation?

On-nuclear spectroscopy with deconvolution of 20 RQ QSOs from the Hamburgh (slitless spectroscopy) QSO survey at z ≤ 0.3 shows (Lewave et al. 2007)

- 66% stellar populations of young Sc-type gals and large reservoirs of gas.
- 50% RQ QSOs in disk-like galaxies, but the most luminous are indeed E gals.
- 75% of E hosts have ionized gas and 50% signs of interactions
-only 15% of S hosts show signs of interactions.

FIR properties of QSOs also indicate SF (Barthel 2006)

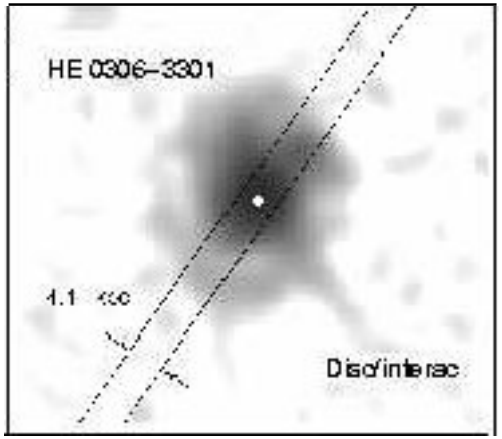

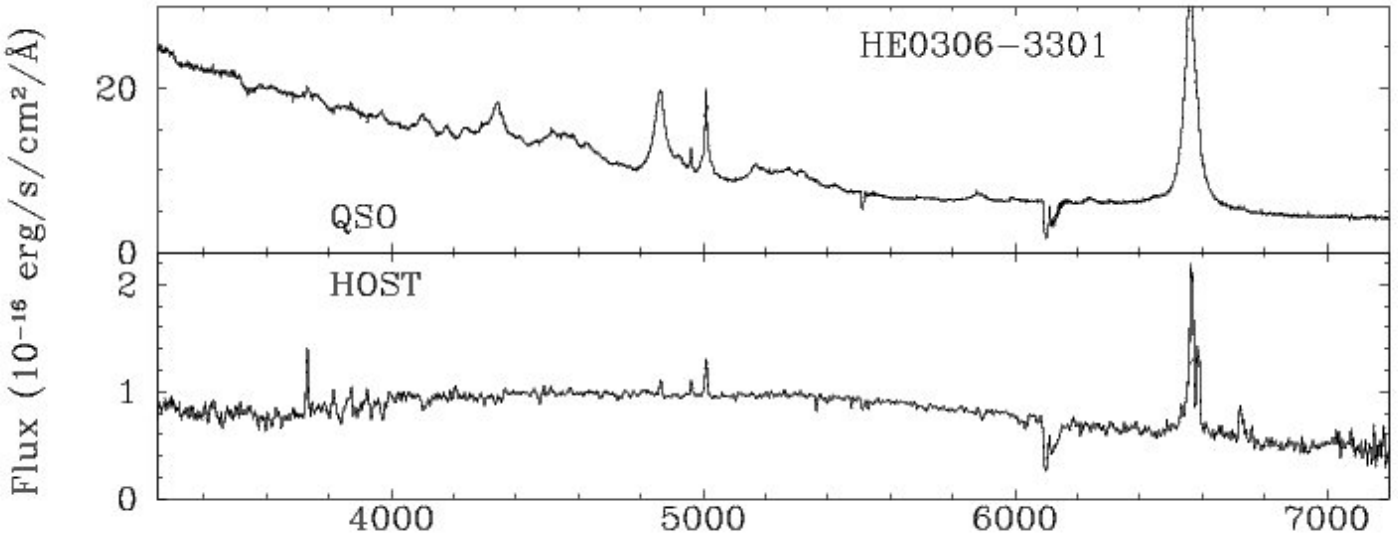

(Lewave et al. 2007)

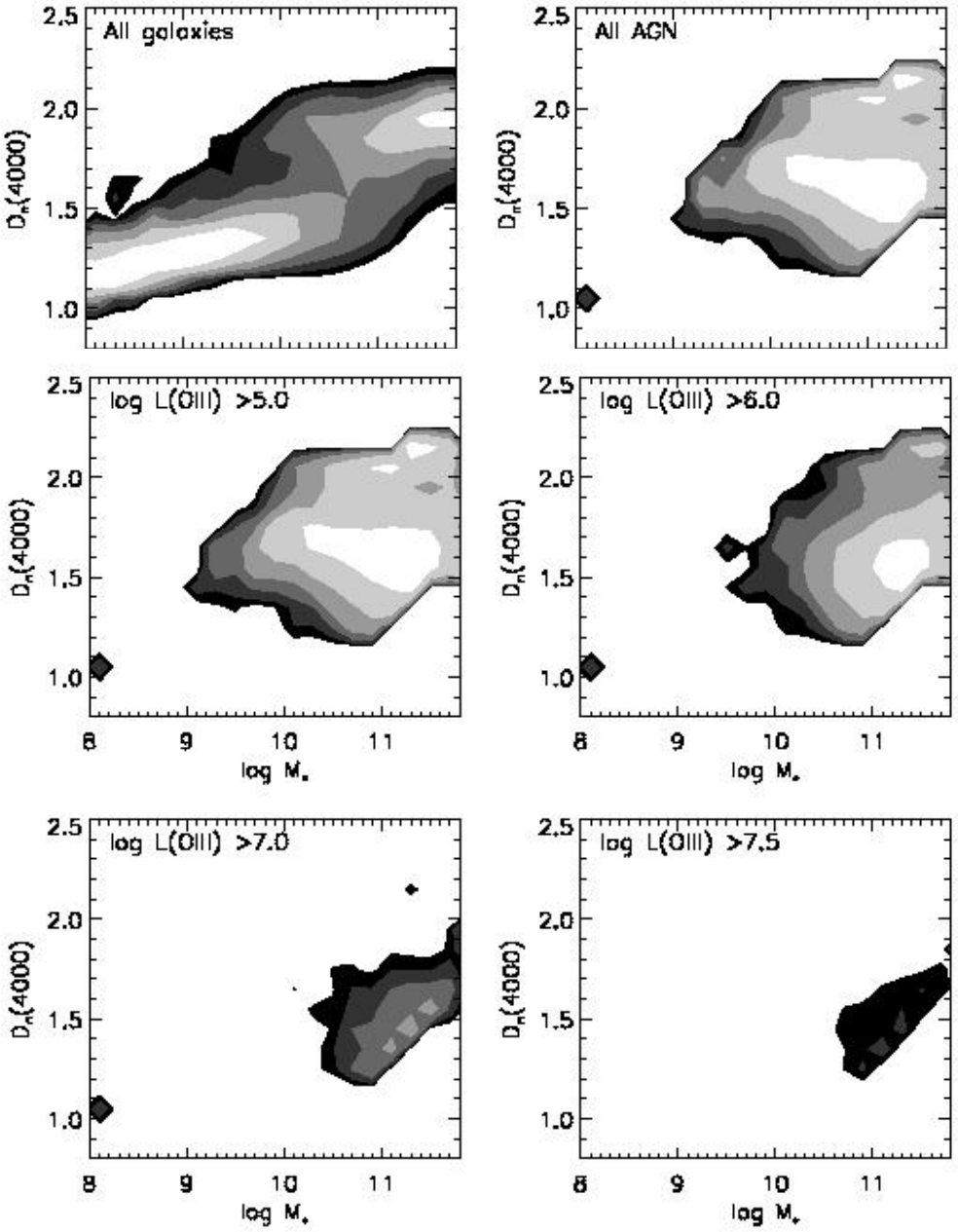

The spectra of 26000 SLOAN narrow-line AGN show that they preferentialy reside in giant galaxies with signs of recent star formation, as revealed by the λ4000Å break measurements (D_n index). The more active the galaxy is (as measured by the [O III] λ5007Å flux), the more massive and young the associated stellar population seems to be (Heckman 2003).

But are these young populations associated with the nucleus or with the host galaxy? — Fiber Φ=3”

Low-*z* QSOs: BH-spheroid relation

The BH-bulge relationship found in nearby galaxies is shared by the AGN where good determinations of the BH mass are available either by reverberation (e.g. NGC 5548) or by rotational curves (e.g. NGC 4258). In a sample of 30 QSOs at $0.1 < z < 0.3$, 19 Seyferts, and 18 inactive S galaxies with reliable bulge luminosities, and applying a M/L relationship, it is found that the masses of BH and bulges are linked by $M_{\rm BH} \propto M_{\rm bulge}^{(0.95\pm0.05)}$

The QSO BHs are radiating at ≤10% of the Eddington limit (McLure & Dunlop 2001)

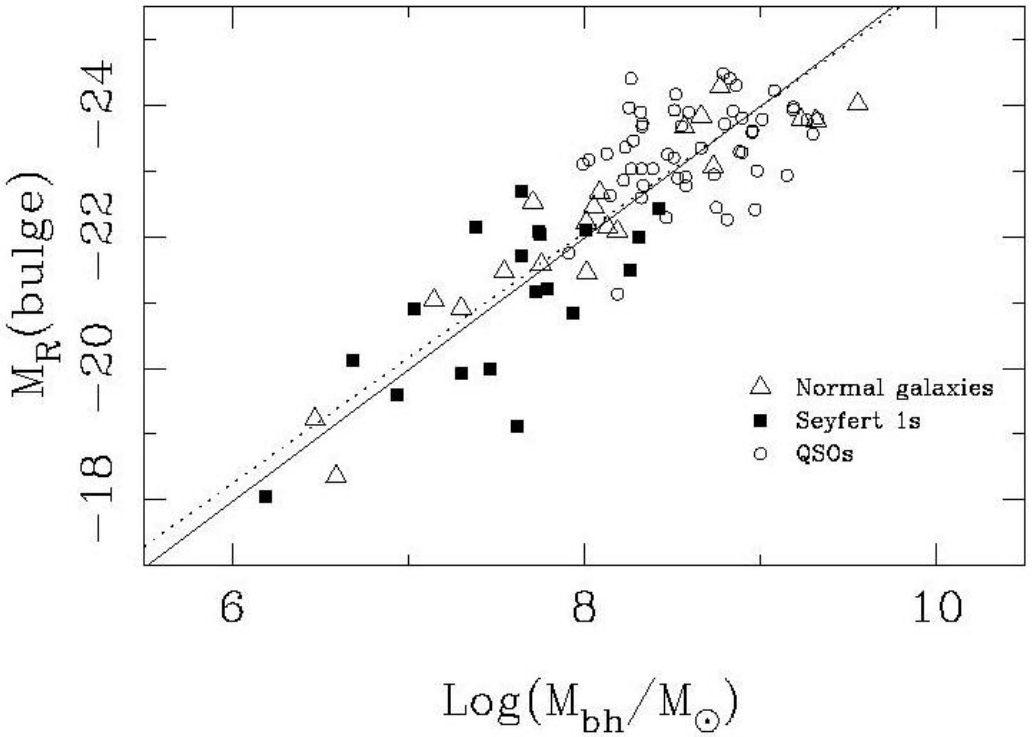

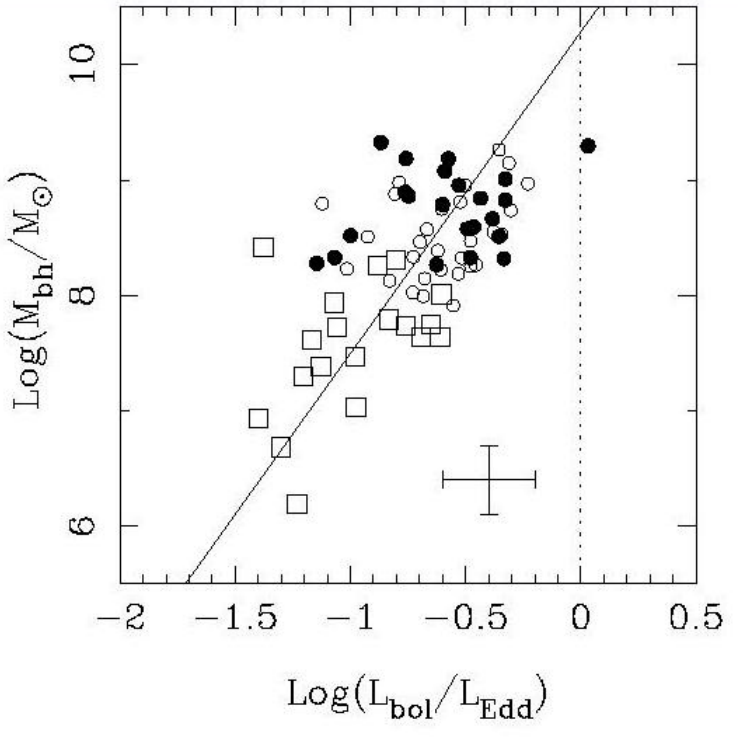

QSO hosts at high-*z*: the building of spheroids

K-band imaging reveals that powerful z≈2–3 RL QSOs (sample of 6, Lehnert et al. 1992) and RQ QSOs (sample of 6, Aretxaga et al. 1998, Falomo et al. 2005, Kuhlbrodt et al. 2005, Kotilainen et al. 2007) follow the same magnitude-relationship as first-rank cluster members. The luminosities are above $3L_*$. These probably become luminous E galaxies. Typical RQ QSOs (sample of 5) seem to be L_* galaxies with a range 0.2−4 L_* (Ridgway et al. 2001). Its nuclear-to-host luminosity is reproduced by semi-analytical galaxy+BH formation scenarios (Ridgway et al. 2001).

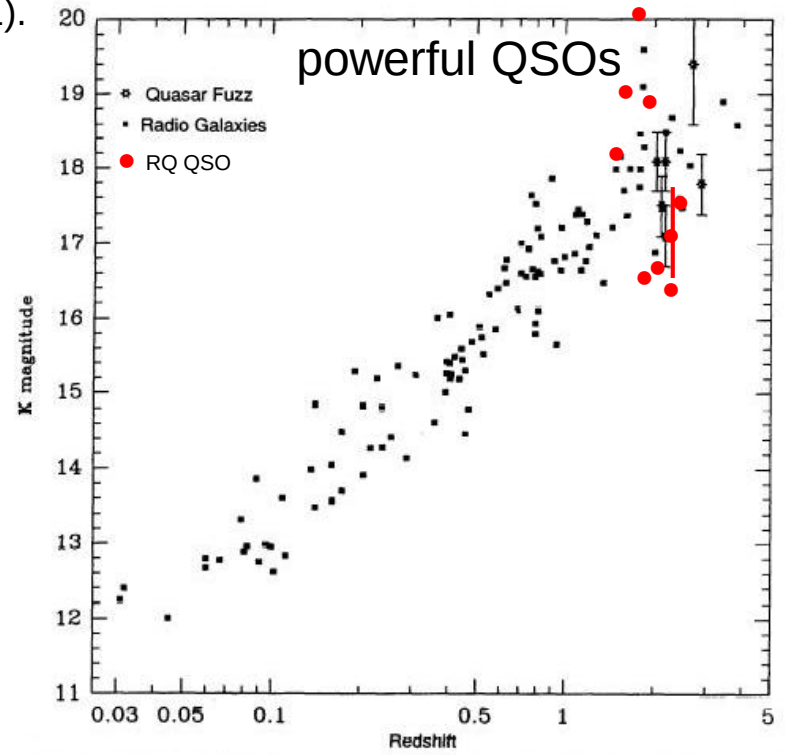

(Lehenrt et al. 1992, Aretxaga et al. 1998)

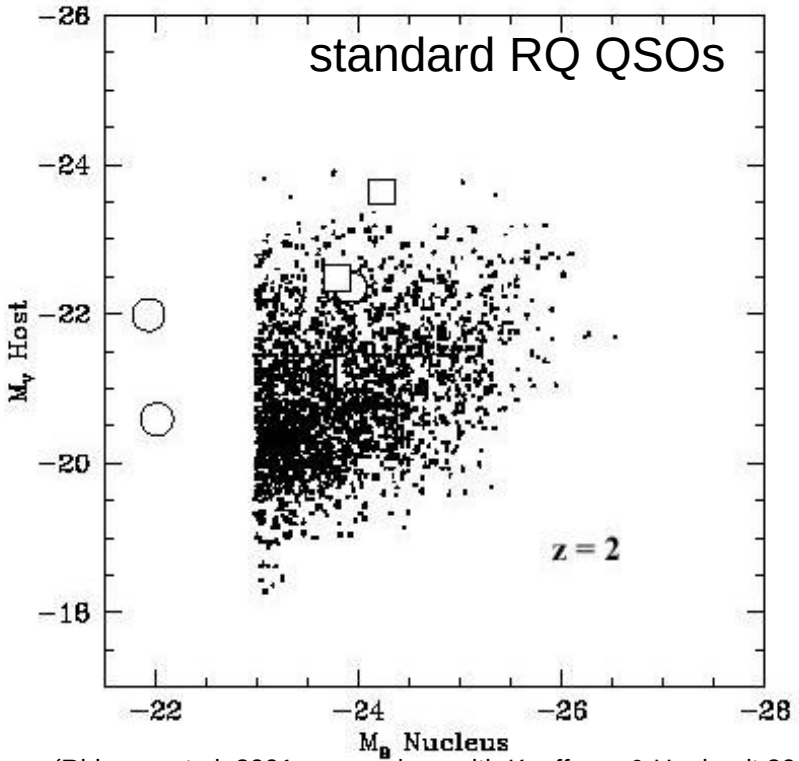

(Ridgway et al. 2001, comparison with Kauffman & Haehnelt 2000)

QSO hosts at high-*z*: the building of spheroids

Photoionization modeling of the BLR in high-*z* QSOs implies that the metallicities of the gas orbiting the engine are typically oversolar (Hamann & Ferland 1993, ...,1999), and this picture extends up to the z≈6 (Pendericci et al. 2002).

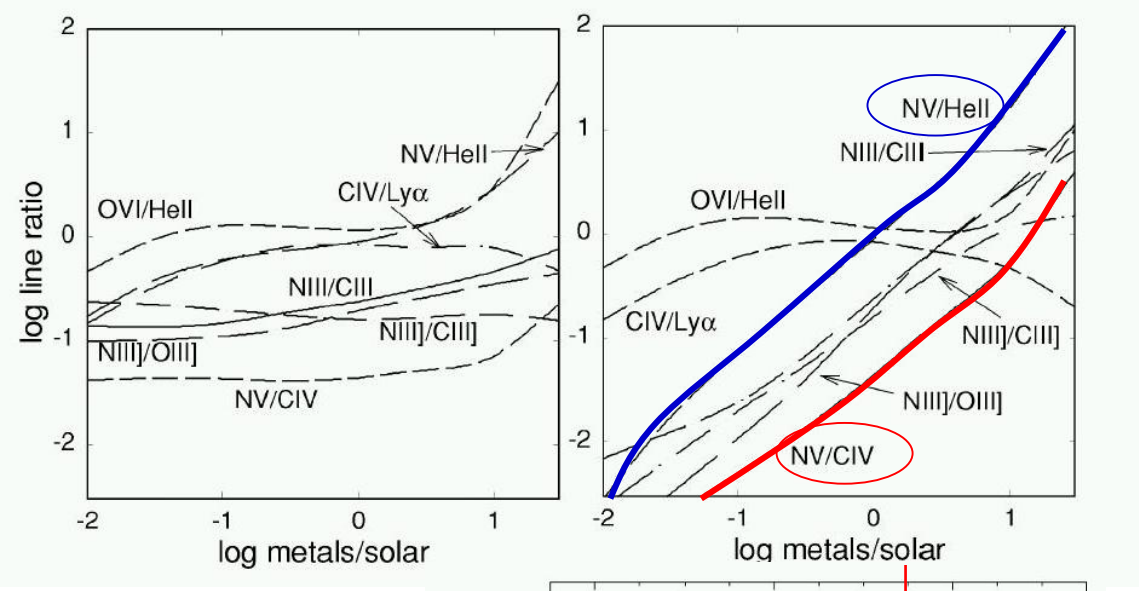

(Hamann & Ferland 1999)

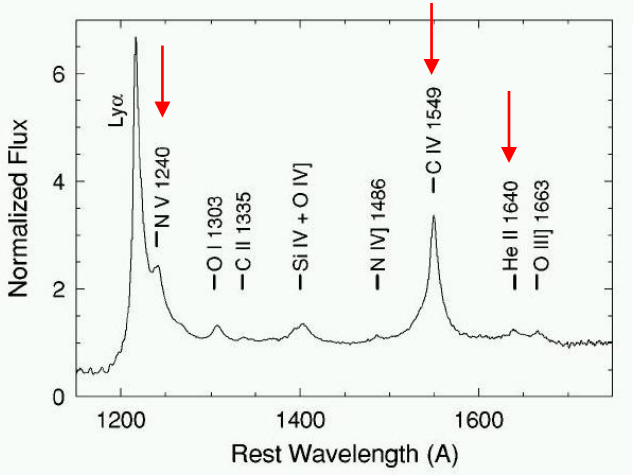

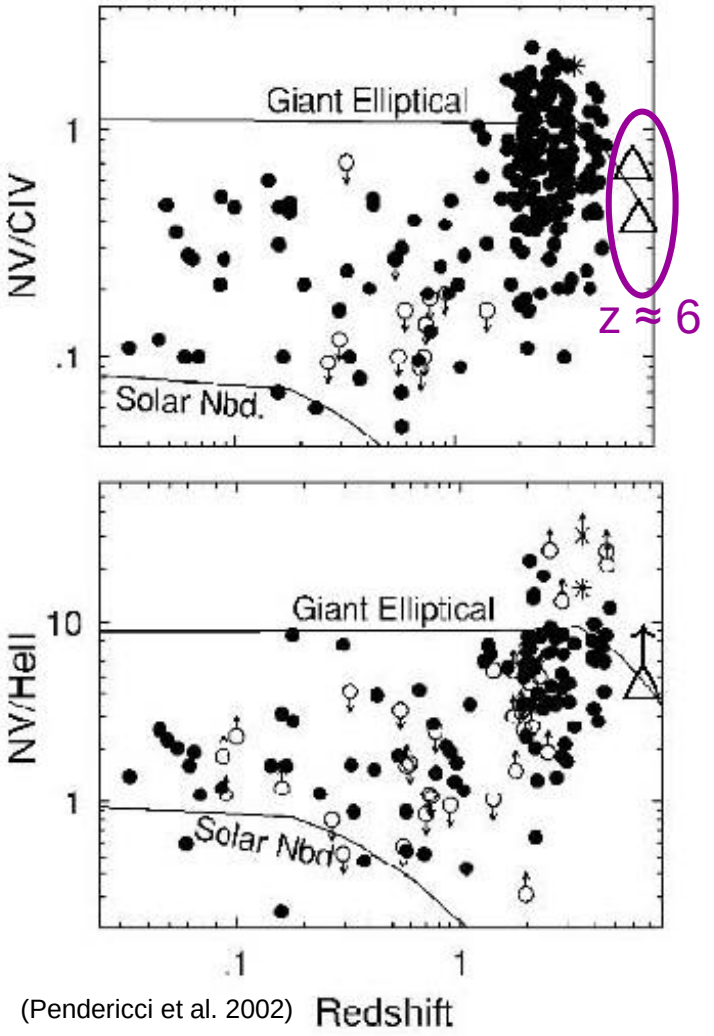

(Pendericci et al. 2002)

QSO hosts at high-*z*: the building of spheroids

Follow-up CO interferometry of the dusty QSOs imply that they contain large reservois of molecular gas $M \geq 10^{10}\, M_{\odot}$ at $z \approx 4$ (Omont et al. 2001). This emission has been resolved in a high-*z* QSO (Carilli et al. 2003).

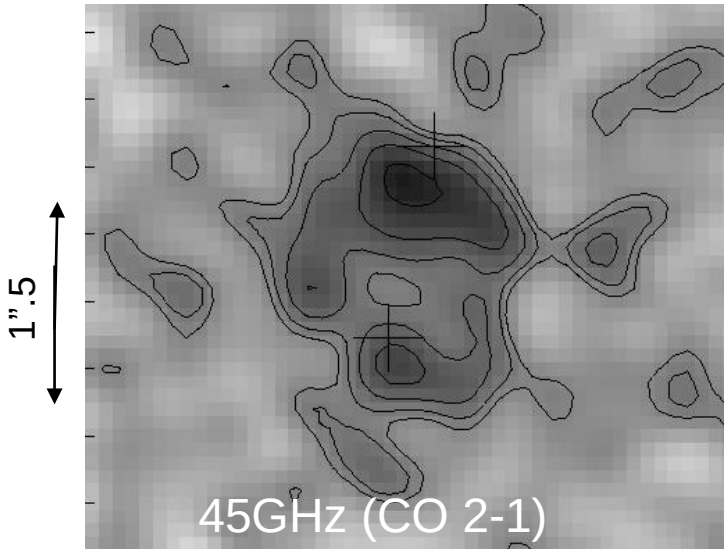

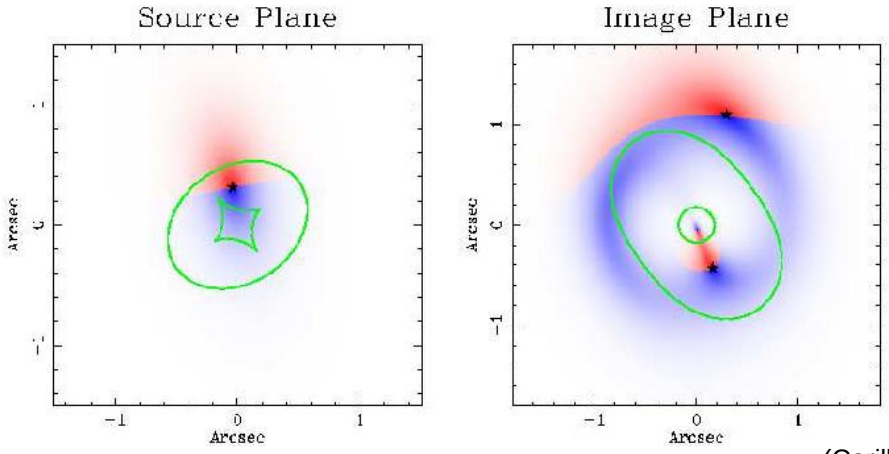

(Carilli et al. 2003)

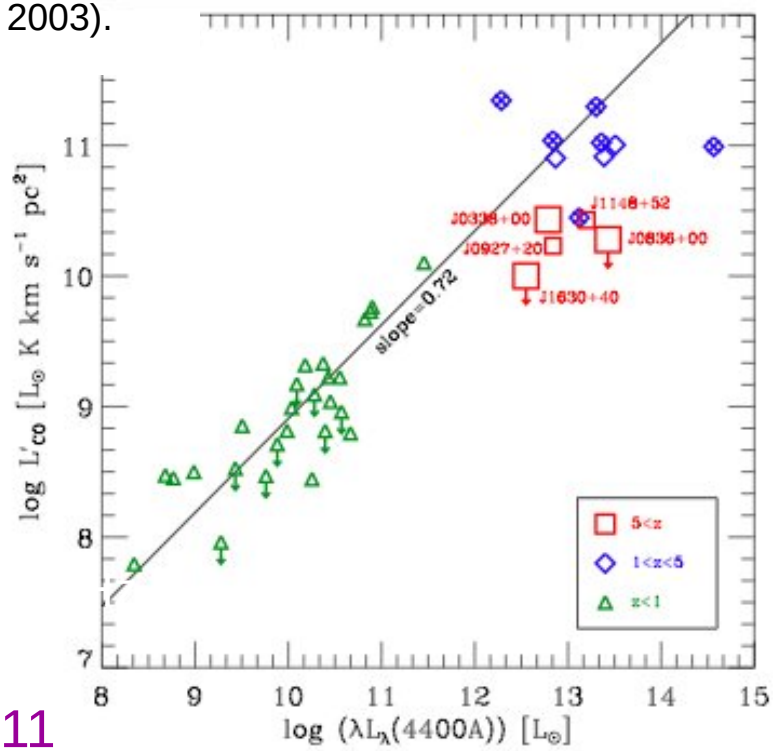

(Maiolino et al. 2007)

$z = 4.11$

M_{gas}=2 x $10^{11}\, M_{\odot}$

$r \approx$2 kpc

SFR ≈ 900 $M_{\odot}$/yr

QSOs in a galaxy evolution context

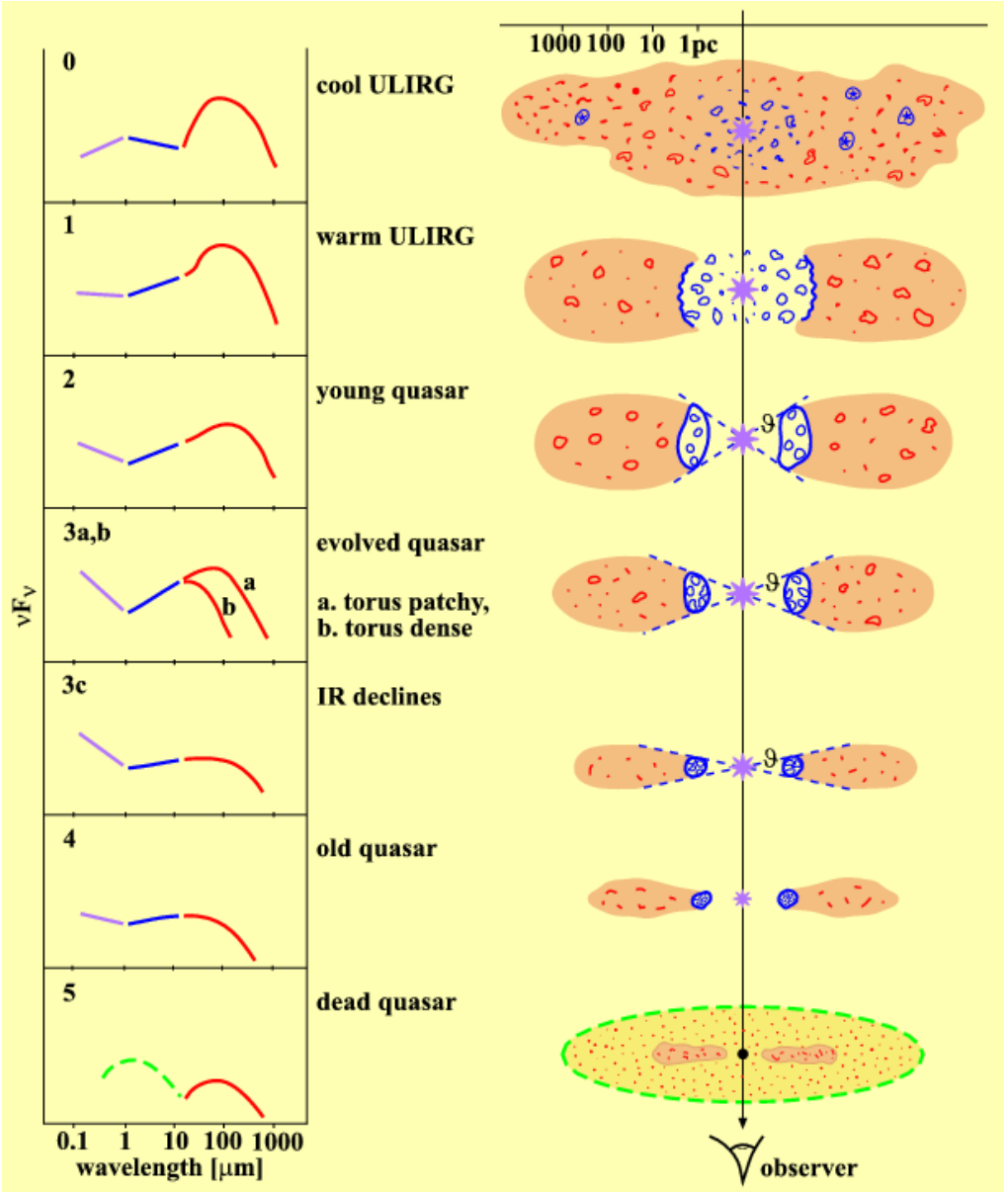

The AGN role in galaxy evolution

The shape of the density evolution of UV light emitted by QSOs also has a similar shape to the density evolution of UV light emitted by field galaxies detected in deep surveys (Boyle & Terlevich 1998).

The LF evolution can be reproduced by models of the growth of BHs and galaxies within the Press-Schechter formalism (Haehnelt et al. 1993, 1999).

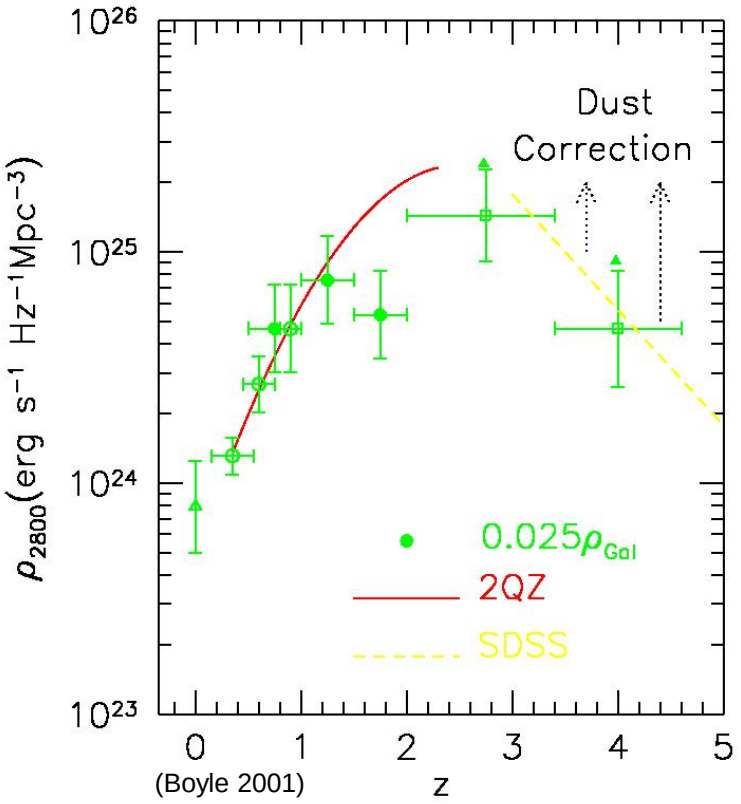

The Press-Schechter formalism is used to obtain the halo mass function $\Phi(M_{halo})$ at any given epoch. This can be related to the BH mass via a BH-halo mass relationship (a la BH-bulge). Assuming a time evolution of the QSO $L(t) = L_E \exp(-t/\tau_Q)$ the LF at z<3 can be reproduced for a range of QSO life-times:

$\tau_Q = 10^6$ yr with $M_\bullet \alpha M_{halo}^{5/3}$ to

$\tau_Q = 10^8$ yr with $M_\bullet \alpha M_{halo}$. However, one needs to assume $M_\bullet/M_{halo}$ α $(1+z)^{5/2}$ or that the mass accretion falls by a factor of 100 (Haehnelt et al. 1999).

The AGN role in galaxy evolution

The shape of the density evolution of UV light emitted by QSOs also has a similar shape to the density evolution of UV light emitted by field galaxies detected in deep surveys (Boyle & Terlevich 1998).

The LF evolution can be reproduced by models of the growth of BHs and galaxies within the Press-Schechter formalism (Haehnelt et al. 1993, 1999).

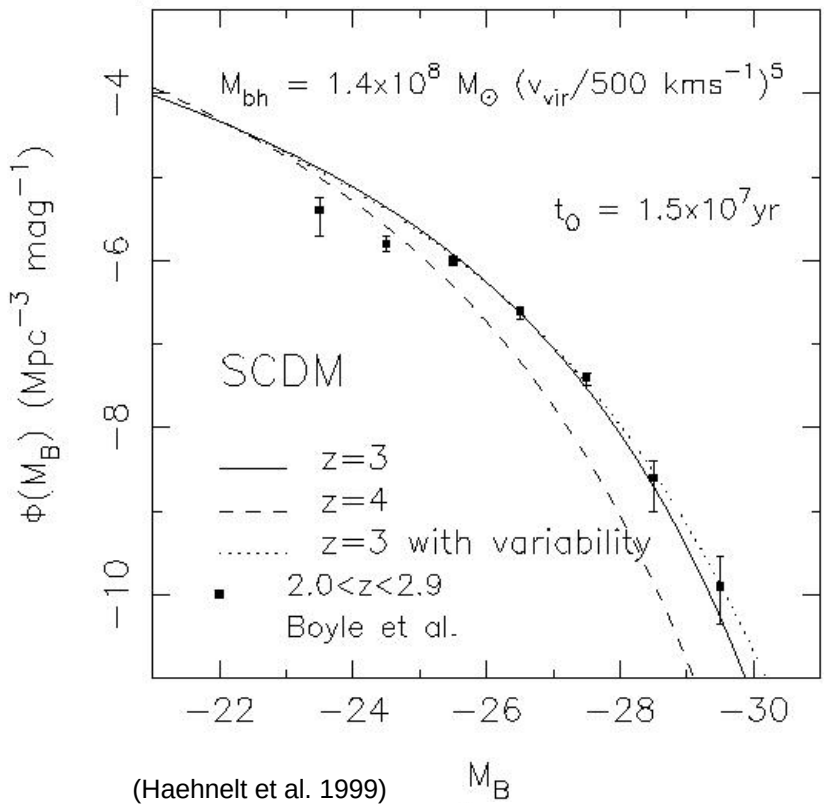

(Haehnelt et al. 1999)

The Press-Schechter formalism is used to obtain the halo mass function $\Phi(M_{halo})$ at any given epoch. This can be related to the BH mass via a BH-halo mass relationship (a la BH-bulge). Assuming a time evolution of the QSO $L(t) = L_E \exp(-t/\tau_Q)$ the LF at z<3 can be reproduced for a range of QSO life-times:

$\tau_Q = 10^6$ yr with $M_\bullet \alpha M_{halo}^{5/3}$ to

$\tau_Q = 10^8$ yr with $M_\bullet \alpha M_{halo}$. However, one needs to assume $M_\bullet/M_{halo}$ α $(1+z)^{5/2}$ or that the mass accretion falls by a factor of 100 (Haehnelt et al. 1999).

Inflows at low-z: feeding the monster

HST F606W images of inner kpc (Simões Lopes et al. 2007) :

- Dusty nuclear spirals in all early-type AGN;
- But in only 25% of control sample;

-> Nuclear spirals correlated with AGN: channels to feed the SMBH (Maciejewski 2004, van de Ven & Fathi 2010; Piñol-Ferrer, Lindblad & Fathi 2012; Hopkins & Quataert 2010)

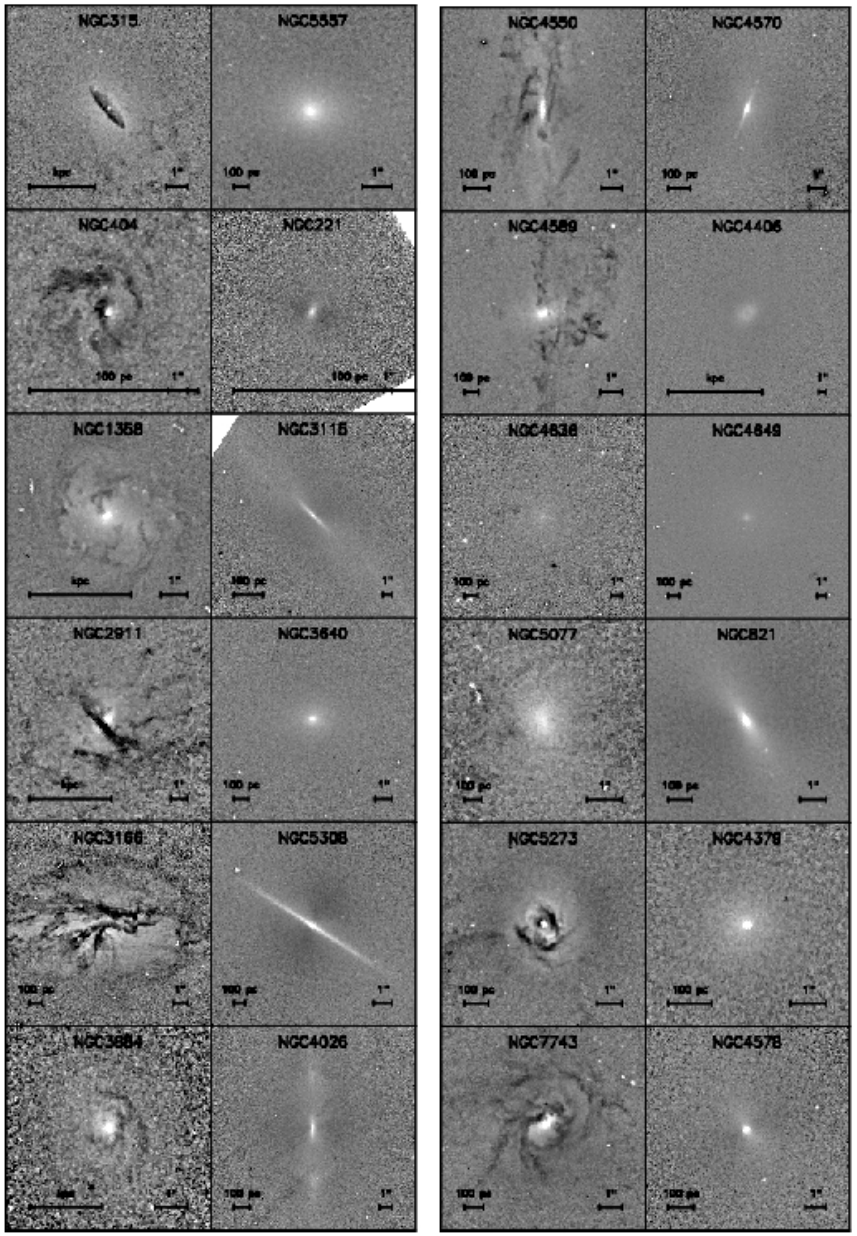

(from T. Storchi-Bergmann´s talk lib)

Inflows at low-z

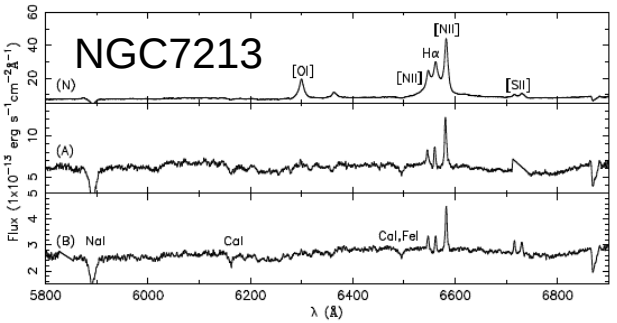

Inflows studied with IFU in 10m-class telescopes
(Schnorr Müller et al.2014,2015,2016)

- Stellar dynamics smooth rotation
- Gas dynamics show Inflows in nuclear spirals, bars and disks, capture of dwarf companions.
- Inflow velocities ~ 100 km/s
- Inflow rates ~0.1 – few $M_\odot yr^{-1}$: 10^2-10^3 times the AGN accretion rate
- Estimated total gas masses in inner kpc ~ 10^7 - 10^9 $M_\odot$
- Surface molecular mass densities: 100 – 7000 $M_\odot pc^{-2}$ -> KS law -> SFR ~ 0.1 – 10 $M_\odot yr^{-1}$

➢ **co-evolution: SMBH at 10^{-3} $M_\odot yr^{-1}$ and bulge at 1 $M_\odot yr^{-1}$**

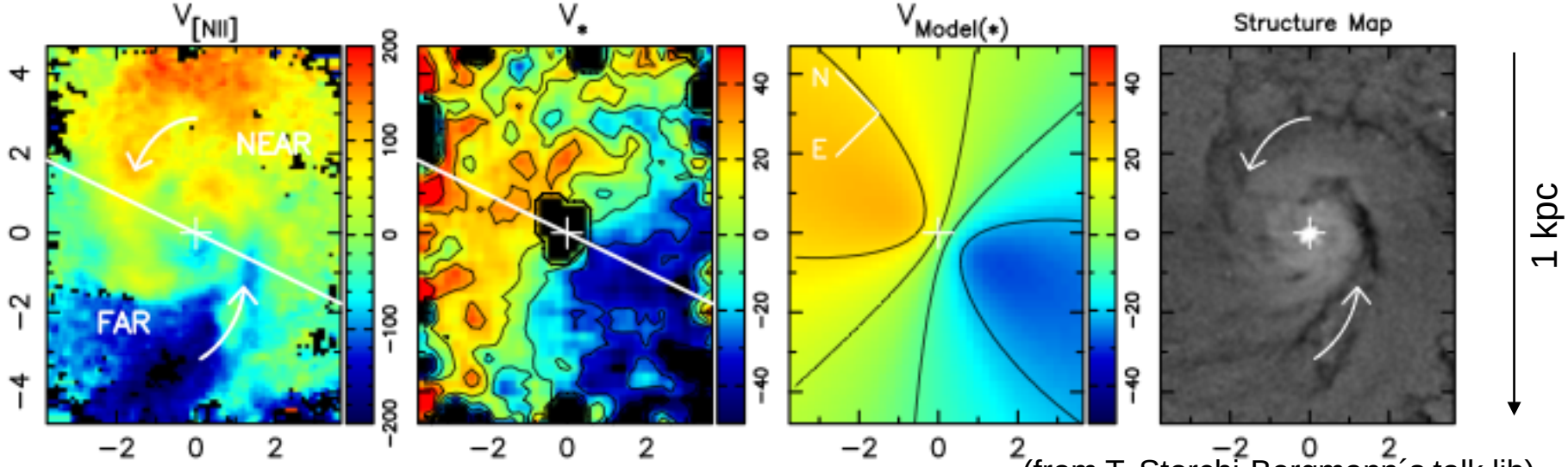

(from T. Storchi-Bergmann´s talk lib)

Outflows at low-z: winds

Identifying the effects of AGN feedback in outflows often relies on observing high velocity (e.g., >500 km/s) components and an outflow power exceeding that predicted for starbursts

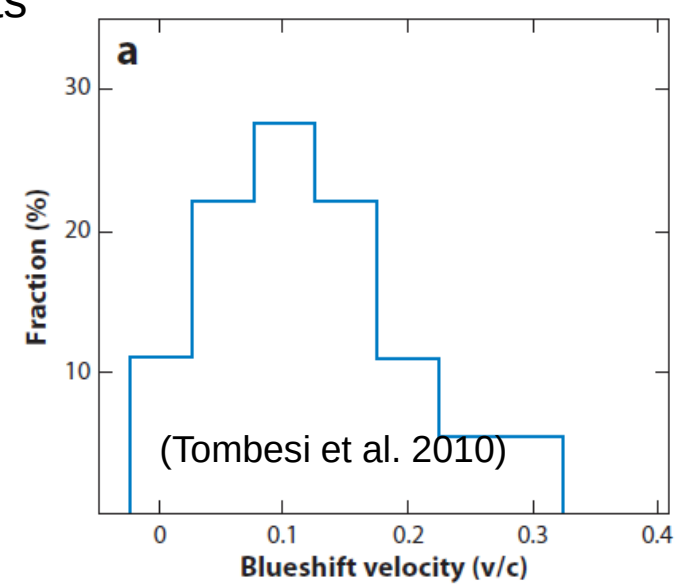

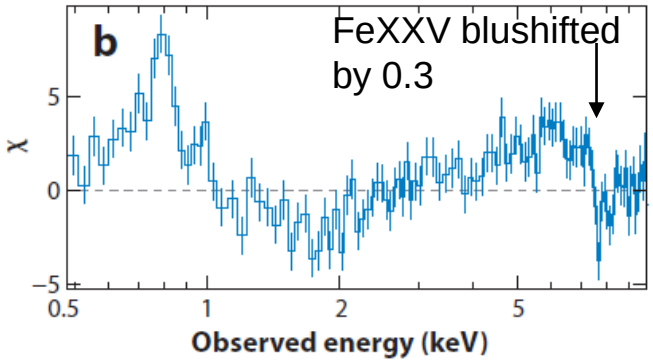

Blueshifted X-ray absorption in PDS 456, at z = 0.184 (Reeves et al. 2009).

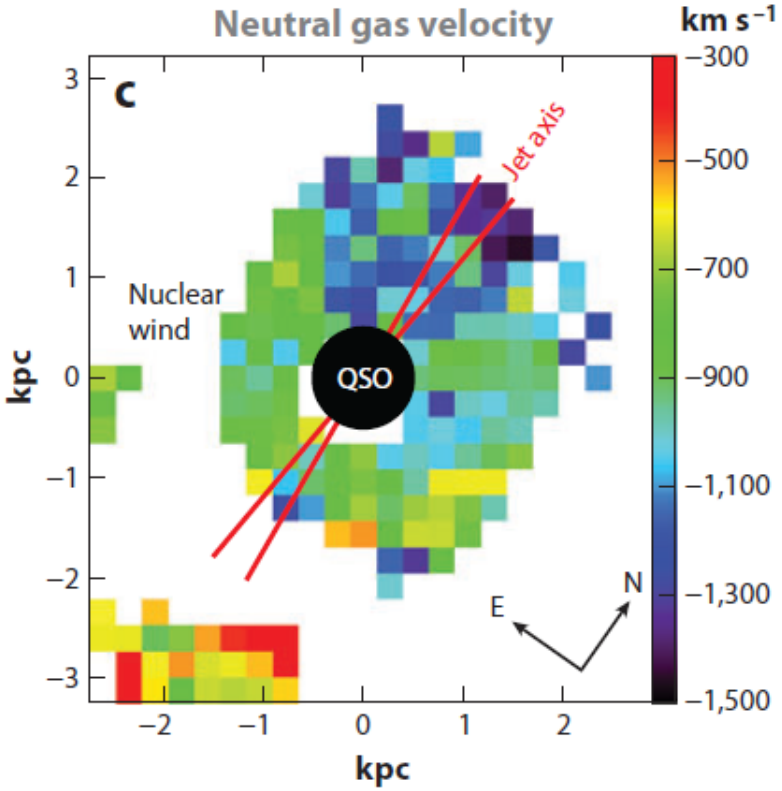

Neutral gas in Mrk 231 with Ejection velocities >1000 km/s and an outflow rate of 420 $M_{\odot}$/yr, larger than the SFR (Rupke & Veilleux 2011).

Outflows at low-z: the effect of jets

Jets can inflate bubbles of relativistic plasma on either side of the nucleus, compressing gas that can lead to star formation.

.

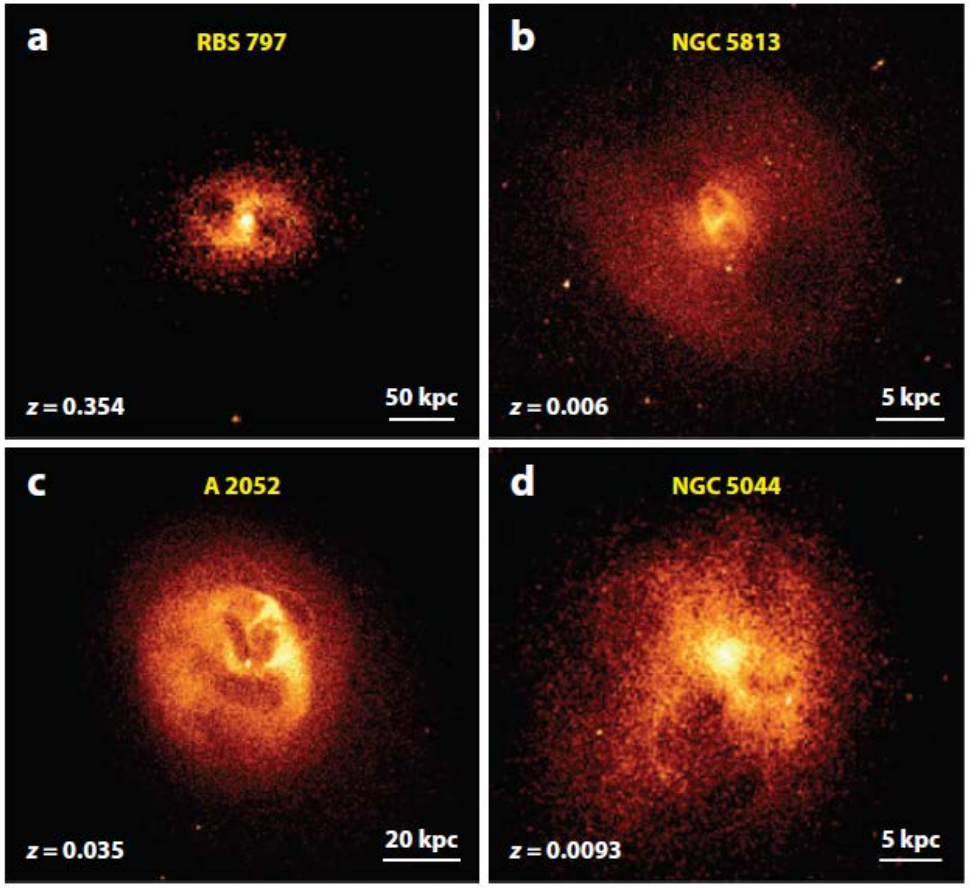

(*a*) Massive cluster RBS 797 at z = 0.354 (Cavagnolo et al. 2011), (*b*) nearby central group elliptical galaxy NGC 5813 at z = 0.006 (Randall et al. 2011), (*c*) rich cluster A 2052 at z = 0.035 (Blanton et al. 2011), and (*d*) NGC 5044 group at z = 0.0093 (David et al. 2011).

Outflows at low-z

Evidence	Quality
High-velocity broad absorption lines in quasars	Strong
Strong winds in AGN	Strong
1,000 km s^{-1} galactic outflows	Strong
Bubbles and ripples in brightest cluster galaxies	Strong
Giant radio galaxies	Strong
Lack of high star-formation rate in cool cluster cores	Indirect
$M-\sigma$ relation	Indirect
Red and dead galaxies	Indirect
Lack of high lambda, moderate N_H, quasars	Indirect
Steep $L-T$ relation in low T clusters and groups	Indirect

(Fabian 2012)

Active Galactic Nuclei

Itziar Aretxaga (itziar@inaoep.mx)

38th ISYA, Tehran, August 2016

Bibliography:

- "An Introduction to Active Galactic Nuclei", B.P.Peterson, 1997, CUP
- "Quasars and Active Galactic Nuclei", A. Kembhavi & J. Narlikar, 1999, CUP.
- "Active Galactic Nuclei", V. Beckmann & C. Shrader, 2012, Wiley-VCH
- "The Physics and Evolution of AGN", H. Netzer, 2013, CUP
- "Advanced Lectures on the Starburst−AGN Connection", 2001, Eds. I. Aretxaga, D. Kunth & R. Mújica, Word Scientific. Includes reviews by B.P. Peterson, R. Goodrich, H. Netzer, S. Collin, F. Combes, R.J. Terlevich & B.J. Boyle.

- Recent reviews: Heckman T. & Best P., ARAA, 2014, 52, 589 The Coevolution of Galaxies and Supermassive Black Holes: Insights from Surveys of the Contemporary Universe

Fabian A., ARAA, 2012, 50, 455: Observational Evidence of Active Galactic Nuclei Feedback